

Latest aspects of earthquake prediction in Greece based on seismic electric signals, II *

P. Varotsos, K. Alexopoulos and M. Lazaridou

Solid State Section, Department of Physics, University of Athens, Knossou Street 36, Athens 165 61, Greece

(Received November 1, 1990; revised version accepted January 31, 1992)

ABSTRACT

Varotsos, P., Alexopoulos, K. and Lazaridou, M., 1993. Latest aspects of earthquake prediction in Greece based on seismic electric signals, II. In: P. Varotsos and O. Kulhánek (Editors), *Measurement and Theoretical Models of the Earth's Electric Field Variations Related to Earthquakes*. *Tectonophysics*, 224: 1–37.

The latest aspects of the physical properties of seismic electric signals (SES) that are used for earthquake prediction in Greece are described. The procedure currently followed for the selection of a site appropriate for the collection of SES and for the electric dipole configuration of such a station are reviewed. The process of constructing a map indicating the seismic areas for which such a station is sensitive is also described. A review of other electrical precursors observed in Greece is given, along with a summary of the newest theoretical models of the generation of SES. The compatibility of these models with the existing data on SES is discussed. Furthermore, a number of unsolved problems are listed, along with suggestions for future experimentation.

1. Introduction

Since 1981, continuous measurements of the electric field of the earth have been carried out in Greece (Varotsos and Alexopoulos 1984a, b). A telemetric network of eighteen stations (via telephone lines) has allowed the real time observation of the electrotelluric variations since 1983. Transient changes in the electrotelluric field, hereafter called Seismic Electric Signals (SES), were found to precede earthquakes. Using these SES, which can be recognized well before the occurrence of an earthquake (EQ) a number of official predictions have already been issued (Varotsos and Alexopoulos 1984 a, b; Varotsos et al., 1986, 1988).

During the past few years the collection of a large body of data has resulted in a new insight into various aspects of the SES earthquake prediction method. We therefore decided to publish two papers reflecting the current state of knowledge: the first paper (Varotsos and Lazaridou, 1991) (hereafter called Paper I) reviewed the latest insights into the basic features of SES (i.e., duration, time lag between SES and earthquake, form, relation between SES amplitude and earthquake magnitude, regional and local characteristics of the selectivity phenomenon, etc.). In addition, a procedure was described by which the epicentre and magnitude of an impending EQ can be determined. Paper I also contained a complete set of predictions issued during the period 1987–1989.

The present paper reviews the following topics: (1) the procedure for the selection of a site appropriate for SES collection; (2) the correct configuration of the electric dipoles in order to

* On the occasion of the 75th birthday of Professor Haroun Tazieff.

discriminate SES from noise; and (3) the procedure for the construction of a map indicating the seismic areas for which a station is sensitive. The basic features of two other types of electrical precursors are presented briefly. In addition, the basic concepts of the theoretical models recently suggested for the explanation of SES generation, are summarized, along with a critical discussion on their compatibility with the experimental results in Greece. Finally, we list some of the numerous questions that still remain and suggest future experiments that could help towards clarifying them.

In order to facilitate the reading of the present paper we first give a short recapitulation of certain points described in Paper I.

The term *SES* is reserved for isolated precursor signals. *Electrical activity* refers to a series of signals that are detected within a period shorter than the time lag between the signal and the ensuing EQ. The (isolated) SES have been found to have a time lag, Δt , which usually varies between 7 h and around 11 d. It has been observed that, although the time lag between the onsets of the electrical and seismic activity does not usually exceed 11 d, the time lag between the largest SES and the strongest EQ can be much longer (up to a couple of weeks). The duration (τ) of an SES is between half a minute and several hours. The time lag and the duration have been found not to depend on the magnitude of the EQ. We define a *signal* as a transient change, ΔV , in the potential difference registered between the electrodes of a dipole. It is evidence of a deviation in the *current density* in the Earth at the location of the dipole. As the dipoles have different lengths (L) the measurement gives the electric field strength, $\varepsilon (= \Delta V/L)$, provided that the surroundings of the station are homogeneous.

The form of a SES can vary; it can have a gradual or an abrupt onset (i.e., with several seconds) and a gradual or abrupt cessation. The combination “gradual onset/abrupt cessation” has never been observed. It should also be mentioned that SES originating from the same seismic area and recorded at the same station occasionally have strikingly similar shapes (waveforms).

1.1. Rules for SES registered at a given station and originating from a given seismic area

In view of the complexity of the experimental data we start with a dipole of given orientation (e.g., E–W or N–S) at a given station. A SES arriving from a given seismic area always has the same algebraic sign, that is, there is always an increase (or a decrease) in the usual field strength, thus giving a characteristic *polarity* for each pair “seismic area–station”.

The relationship between the SES amplitude expressed as $\Delta V/L$ (Usually ΔV in millivolts and L in metres) and the magnitude M has been found to be:

$$\log(\Delta V/L) \approx (0.34-0.37)M + b$$

which gives a straight line plot with an intercept, b . The plots for dipoles of two orientations have the same slope (0.34–0.37) but different intercepts. This means that the ratio of the amplitudes $(\Delta V/L)_{EW}/(\Delta V/L)_{NS}$ remains the same and is characteristic of all EQs predicted from SES recorded at a given station and coming from a given seismic area.

1.2. Rules for SES registered at a given station and originating from different seismic areas

A given station, S_A , situated at A may be able to record SES originating at seismic area B but not at area C , even if $r_{AC} < r_{AB}$. This effect, called *selectivity*, is not reversible, in the sense that, although station S_A can record signals from seismic area B , station S_B , situated at B , does not necessarily record signals from seismic area A .

The selectivity effect is not solely a directivity phenomenon; a station, S_A , may be able to feel a signal originating from B but not from C , although all three points lie on a straight line and the distance r_{AC} is smaller than r_{AB} . Various observations indicate that selectivity depends simultaneously on: (1) the physical properties (e.g. conductivity) of the *path* between the station and the seismic area; (2) the *source properties*, for example, the directional properties of the emitted current; and (3) the *inhomogeneities* in the vicinity of the station.

In spite of the complexity of the selectivity effect, a SES is reproducible in time and space in the sense that once a station has been found to be sensitive to SES from a given area, it will be so for all future earthquakes.

1.3. Procedure for the determination of the epicentre

The epicentre can be determined from SES data using various criteria. These depend on the number of stations that have detected a certain signal. Under the present configuration of the network, the SES of an impending EQ is usually registered only at one station so that the epicentre has to be determined from a single data set.

Let us assume that the SES was recorded at a single station, S_A , and no simultaneous SES traces were recorded at any other station. The following effects are then considered in order to exclude certain regions and determine the epicentral area by a process of elimination:

(1) Selectivity effect. Using earlier experience, we can exclude as possible epicentral regions areas for which the station is not sensitive. This leaves us with a restricted set of seismic areas: only those that have either already produced SES recorded only at the station S_A or a new seismic area. A “new” area is defined as one which has not been active since the installation of the SES recording station.

(2) Polarity effect. From the above restricted set of seismic areas it is also possible to exclude those known seismic areas to which station S_A is sensitive but which emit SES with polarity component(s) opposite to those of the signal recorded.

(3) Ratio of the two components of the SES. After the ratio $(\Delta V/L_{EW})/(\Delta V/L_{NS})$ of the signal in question has been determined, it can be compared to the corresponding ratios of SES formerly collected from the seismic areas that remain after exclusions based on (1) and (2). It is clear that the identification of the epicentre is straightforward for seismic regions which have been active in the past, so that this ratio is known. A difficulty arises when the ratio for the signal under consideration does not coincide with any known value. In such a case, a less reliable

prediction of the expected epicentral area may be achieved by interpolating values from neighbouring areas. Sometimes it is preferable, instead of the aforementioned ratio, to use the ratio of the quantity $\Delta V/L$ of a long dipole (with an intermediate direction, i.e. not exactly E–W or N–S) over $\Delta V/L_{EW}$ (or $\Delta V/L_{NS}$) of a short dipole.

1.4. Magnitude determination

After the epicentral area has been predicted the magnitude can be estimated as follows: Let us assume that data from the recording station S_A leads to the conclusion that the expected epicentre lies within the seismic area B . Earlier data from station S_A for earthquakes in this particular seismic area have provided linear plots of $\log(\Delta V/L)$ versus M for the dipoles in each direction. These two plots and the corresponding amplitudes ($\Delta V/L$) of the two components of the new SES provide an estimation of the magnitude of the impending event. Therefore, for an accurate estimate of M for a future earthquake from data collected at a single station, a “calibration” of the station must be available for each seismic area to which it is sensitive. The collection of such data requires long periods of recording. However, since the plots of $\log(\Delta V/L)$ versus M always have a slope between 0.34 and 0.37 a single clear SES is enough for calibration.

2. Selection of sites appropriate for SES collection

In view of the local and regional characteristics of the selectivity effect described in Paper I, the selection of a site for a permanent installation is a tedious task. We stress that even if we select a site that exhibits extremely low industrial noise it may not be appropriate for SES collection. We are aware of a number of such low noise sites in Greece where portable stations were intentionally operated for several years without having recorded even one SES. Since, during this period of continuous operation, a significant number of EQs did occur in various seismic areas of Greece, we determined some low-noise sites (hereafter called insensitive sites) that did not record any

SES from the seismic areas that became active during the period of experimentation.

Apart from a geological and geotectonic inspection, the installation of a station appropriate for SES collection should *necessarily* be preceded by an investigation which includes the installation of a number (e.g., 10) of temporary low noise stations a few kilometers apart. Only after the occurrence of a few significant events from a given seismic area (*A*), for which the preceding SES were recorded, can we select the most appropriate of these stations for further investigation of area *A*. For each temporary station the technique shown in Figure 1 can be used. That is illustrates the procedure for such an investigation. A telephone cable several kilometers long and comprising a significant number of wires (e.g., 16) is used for testing a number of sites. Each wire leads to an electrode at a different

point so that potential differences between points with distances lying from, for example, 100 m to several kilometres can be measured.

The above procedure has already been applied in Greece for the determination of a number of "sensitive points" at which the permanent stations shown in Figure 2 were installed. These sites were chosen in order to obtain stations selective to the seismic areas active at the time. The operation of such a station for a period during which several seismic areas were active enabled the construction of a selectivity map for this station (see below). The following two points should be emphasized:

(1) After having found a suitable site for a station selective to a given seismic area, no general rules exist for the prediction of other seismic areas for which this site is appropriate for SES collection. This is due to the fact that, as ex-

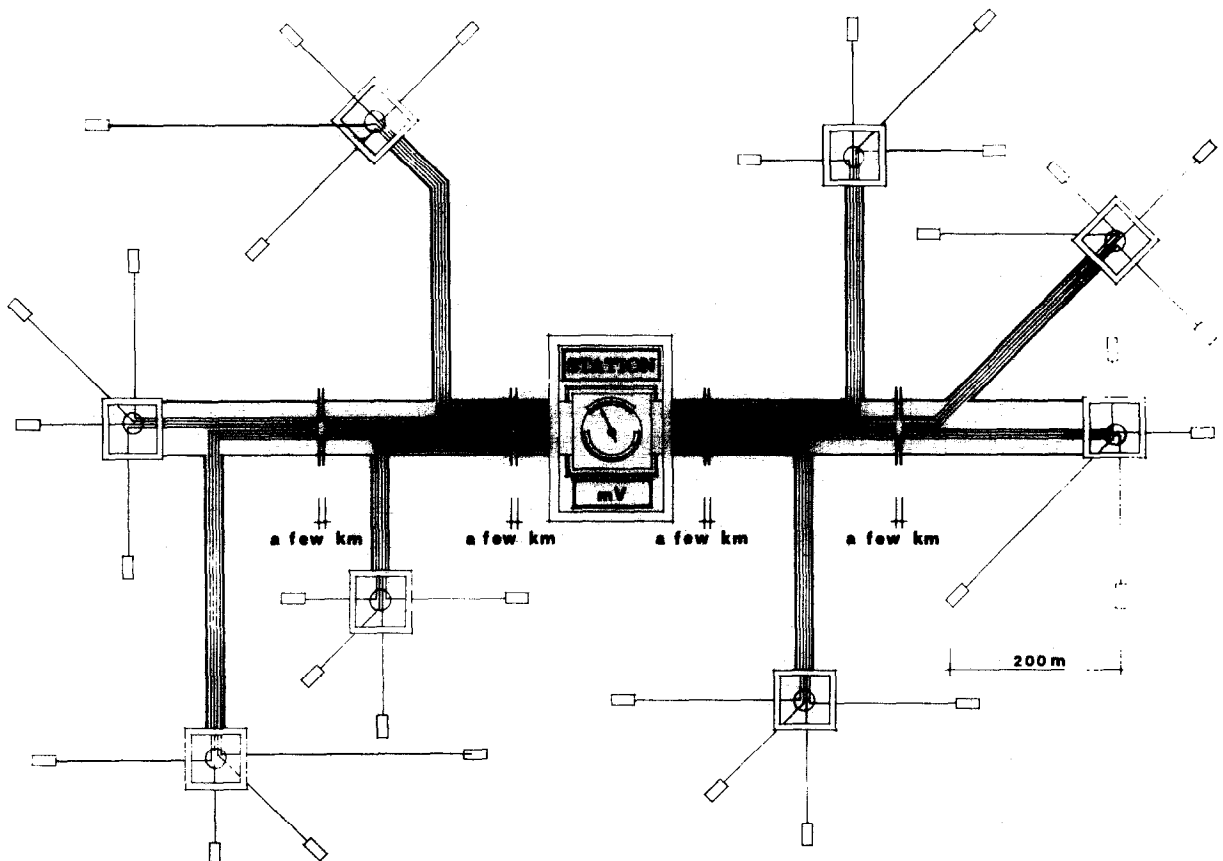


Fig. 1. Schematic representation of the electrode installation at a temporary station in order to investigate a number of neighbouring sites simultaneously. The 16 wires of a telephone cable lead to electrodes. At the station a system of differential amplifiers measures the potential differences of various pairs of these electrodes.

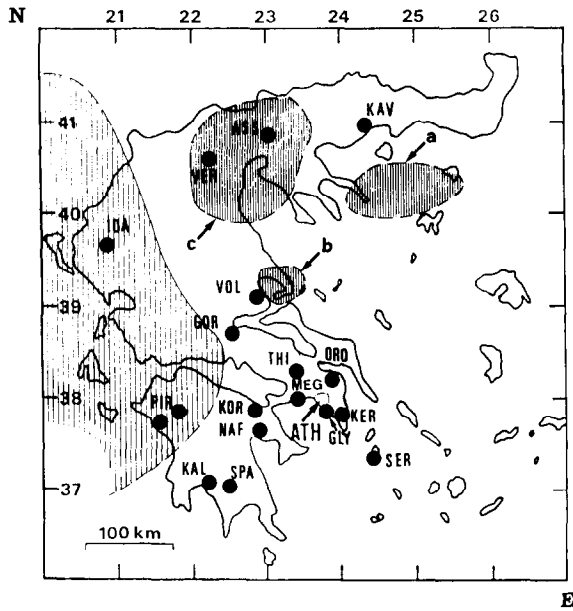


Fig. 2. Selectivity maps of the stations ASS and IOA. The sites of the other Greek stations are also shown. The areas *a*, *b* and *c* correspond to seismic areas from which SES are solely collected at station ASS. The large hatched area is the selectivity map of station IOA and includes seismic areas from which the SES are collected either at station IOA alone, or at station PIR as well. The signals at PIR are restricted to the Cephalonia region or to neighbouring areas of station PIR, but oriented in a SW-NE direction (Varotsos and Alexopoulos, 1984a, b).

plained in Paper I, the selectivity is not purely a directivity effect, but simultaneously depends on the "source properties", the "travel path" and the inhomogeneities close to the station.

(2) It is known that a magnetotelluric (MT) study of an area leads to the understanding of its geoelectrical structure. However, although this structure was found to play a significant role (see Paper I) it is not the sole factor governing the suitability of a site for the detection of SES from a given seismic area. In other words, an MT investigation does not provide a unique tool for the selection of a site appropriate for SES collection from a given seismic area.

This can be explained (within the frame of the model predicting currents originating at the focal area) as follows: let us take two sites, *A* and *B*, belonging to two different areas and a remote seismic area *C*. Even if we assume that the geoelectrical structure below *A* and *B* is practically the same, the following situation could occur: a

channel could "drive" the SES emitted from the focal area *C* to one of the two sites but not to the other.

In view of the above aspects, it seems necessary (at least at the present stage of our knowledge) that the suitability of a site for SES collection from a given seismic area should be carried out on empirical grounds, that is, by long experimentation; for example, with a technique similar to that shown in Figure 1.

The question still remains as to the (broad) area where SES prospection (as shown in Fig. 1) should start. Although general statements cannot be made, it seems that the following three "types" of areas have the most potential:

(1) The vicinity of a major fault: as an example we refer to station ASS, which lies close to a major fault and, although installed on sediments, is selective for a number of seismic areas (Fig. 2). It seems that a fault provides a conductive driving channel for SES propagation.

(2) Regions of crystalline rocks close to large heterogeneities, such as geological contacts with significantly different conductivities. This is the case for station IOA (fig. 25, Paper I), which is sensitive to a significant number of seismic areas (Fig. 2). Note that the good response of station IOA does not seem to be associated with the existence of any major fault in its vicinity.

(3) Area with strong local inhomogeneities. The dykes around station KER, discussed in Paper I, seem to provide appropriate localities for further SES investigations. Note also, that station KER also does not seem to be in the vicinity of any major fault.

3. Appropriate configuration of the dipoles of a station

3.1. Type of electrodes

The current configuration of our network involves non-polarized Pb/PbCl₂ electrodes at a depth of 2 m. However, various metallic electrodes (e.g., copper and brass) and non-polarized ones (e.g., Cu/CuSO₄) have been tested in the past. Although their noise, as expected, was found to be different, we have verified that SES were

collected with all these types of electrodes. Simultaneous recordings at parallel short dipoles of the same length but with different types of electrodes has undoubtedly shown that the same ΔV value for a given SES is recorded. This result indicates that the appearance of an SES cannot be associated with "small scale electrokinetic phenomena" down to the size (and in the neighbourhood) of the electrodes.

The following experiment, among others, was also carried out: two parallel (almost) vertical dipoles, the first one with Cu electrodes and the other with Pb/PbCl₂ electrodes, were intentionally installed close to a dyke in station KER (for the influence of the local inhomogeneities on the SES collection see Paper I). In spite of their small length (a few metres, we found that both dipoles (of equal length) recorded the same ΔV value for a given SES. Note that these dipoles were well above the water level, so that electrokinetic phenomena due to a water diffusion process (induced by a local pre-seismic variation in strain) can be excluded. We shall return at this point.

3.2. Appropriate number of dipoles

The number of dipoles should be sufficient in order to separate true SES from the various types of noise.

As mentioned in Paper I, the noise can be classified into three main categories: magnetotelluric (MT) disturbances, electrochemical variations of the surface of electrodes and cultural (or anthropogenic) noise. The MT noise can be subtracted from the electrotelluric records after having determined, for each site, the impedance tensor, Z , that relates the variations in the magnetic and electric field. A procedure for the "real time" subtraction of the MT noise from our records has already been developed and tested with satisfactory results (Hadjiioannou et al., this issue). Therefore, in the following we shall emphasise the difficulties and the shortcomings that arise from the other two types of noise, which depend on the configuration of electric dipole arrays:

(1) *Two perpendicular short dipoles* (usually in the directions E–W and N–S). This is the config-

uration mentioned in numerous previous papers. It cannot eliminate anthropogenic or electrochemical noise (see Paper I).

(2) *Four short-dipole configuration*, that is, two parallel short dipoles with different lengths in each of the two directions E–W and N–S. Such a configuration excludes the electrochemical disturbances, but suffers from the following serious shortcoming: when a noise source lies at a distance from the station appreciably larger than the length of the short dipoles (fig. 12, Paper I), its disturbances obey the rule $\Delta V/L = \text{constant}$ for each direction and thus can be misinterpreted as SES.

(3) *Configuration involving only long dipoles* (with L of the order of several kilometres). This configuration is achieved using underground telephone lines (Varotsos and Alexopoulos, 1986); in view of the length of the resulting dipoles, electrochemical disturbances do not create significant problems; however, difficulties arise in the interpretation of the data. The following is just one example: the SES of two EQS of equal magnitude and equal epicentral distances but coming from different seismic areas, when recorded at the same long dipole are not necessarily collected with equal ΔV values; according to our experience, this may happen when these two seismic areas give SES with different $\Delta V_{EW}/\Delta V_{NS}$ ratios on the short dipoles of equal length L (see Paper I).

(4) *Configuration including short and long dipoles*. To the best of our knowledge, this is the most appropriate configuration for SES collection and is currently used in our network. By recalling the aspects of Paper I concerning the discrimination between anthropogenic noise and true electrotelluric disturbances (i.e., between SES and MT) we conclude that at least five dipoles must be installed at each station: two parallel short ones in each direction (i.e., E–W and N–S), with different lengths and (at least) one long one. Attention is drawn to the fact that the two electrodes of the long dipole should be placed at sites with the configuration shown in Figure 21. Note that when the long dipole lies in an intermediate direction (i.e., not exactly E–W or N–S) the installation of a sixth electric dipole is highly

recommended; this latter dipole should be a short one and parallel to the long dipole for the reasons explained in Paper I: when a short dipole lies parallel to a long dipole and is directed towards a source of noise then (if the distance between the electrodes and the noise source is, at most, of the same order of magnitude as the length of the long dipole) this noise can be immediately excluded, because its values at these two dipoles violate the condition: $\Delta V/L = \text{constant}$.

The following point should also be borne in mind: when a noise source operates continuously (thus contaminating the records), its influence can be permanently eliminated by the technique described in Paper I.

3.3. Conclusion

Our experience indicates that, when only short dipoles are used, the resulting number of disturbances (i.e., those remaining after excluding electrochemical and MT noise and applying the rule $\Delta V/L = \text{constant}$) usually exceeds, on average, the number of true SES by more than one order of magnitude. An electric disturbance is classified as a SES after it has met *all* four criteria mentioned in appendix 2, Paper I. Therefore, when using only short dipoles, it is usually difficult to establish any correlation between the SES and EQs that occurred in a given seismic area; such a correlation can be attempted only after the additional use of properly installed long dipoles (i.e., as indicated in Appendix II).

4. Construction of a selectivity map

The procedure that should be followed in order to construct selectivity maps is described here. These maps show the seismic areas that emit SES detectable (for EQs above a magnitude threshold of course) at a given station. By recalling the definition of the selectivity effect, it is obvious that each station has its own selectivity map. The following remarks may be useful:

(1) only when a seismic area happens to lie in a region overlapping the selectivity maps of two remote stations can it give SES that are *simultaneously* recorded at these two stations;

TABLE 1

List of earthquakes with SES collected at station ASS

| Date (DD-MM-YY) | Time | Epicentre (°N, °E) | Magnitude (M_s) |
|--------------------|-------|-----------------------|------------------------|
| 10-10-83 | 10:17 | 40.3, 25.5 | 5.7 |
| 23-01-84 | 10:27 | 40.9, 23.3 | 4.3 |
| 07-02-84 | 18:28 | 40.7, 22.2 | 4.4 |
| 19-02-84 | 02:53 | 40.6, 23.4 | 4.3 |
| 19-02-84 | 02:54 | 40.6, 23.3 | 4.3 |
| 19-02-84 | 03:47 | 40.6, 23.4 | 4.8 |
| 19-02-84 | 04:00 | 40.7, 23.4 | 4.2 |
| 04-05-84 | 02:52 | 40.8, 23.4 | 4.4 |
| 08-05-84 | 05:04 | 40.4, 22.8 | 4.8 |
| 08-05-84 | 08:08 | 40.5, 22.8 | 4.2 |
| 14-05-84 | 18:18 | 40.3, 22.7 | 4.5 |
| 15-05-84 | 04:35 | 40.3, 22.8 | 4.3 |
| 14-11-84 | 14:54 | 40.7, 23.5 | 4.4 |
| 30-04-85 | 18:14 | 39.3, 22.9 | 5.3 |

(2) in view of the first remark it is evident that when the selectivity maps of two stations (*i*) and (*j*) have no common area, no simultaneous SES can be recorded at these two stations. This is the case for the two stations ASS and IOA which, during 8 years of continuous operation (1982–1990) have never recorded even one simultaneous SES. This fact cannot be misinterpreted as being due to insufficient experimental data since a number of large events (i.e., close to M_s 6.0) at comparable epicentral distances from each of these two stations but different azimuths (Tables 1 and 2) happened to occur. In order to clarify this case better the following should be considered: Let us take some earthquakes that occurred at epicentral distances of the order of 150–200 km from station IOA with various azimuths locations shown in Fig. 3: *a*, $M_s = 6.0$ on February 11th, 1984; *b*, $M_s = 5.6$ on January 1st, 1988; *c*, $M_s = 5.9$ on May 18th, 1988; *d*, $M_s = 6.0$ on October 16th, 1988; and *e*, $M_s = 5.9$ on August 20th, 1989 (Fig. 3, Table 2). All these EQs gave clearly detectable SES at station IOA. (Figs. 4–10), which means that this station is able to collect SES emitted from significant EQs at comparatively large epicentral distances. In contrast EQ *g* (i.e., the $M_s = 5.8$ EQ on April 30th, 1985), although lying at an epicentral distance more or less comparable to the earthquakes mentioned above, did

TABLE 2

List of earthquakes with SES collected at station IOA

| Date (DD-MM-YY) | Time | Epicentre (°N, °E) | Magnitude (M_s) |
|--------------------|-------|-----------------------|------------------------|
| 08-09-83 | 22:05 | 38.0, 21.2 | 5.4 |
| 11-02-84 | 08:02 | 38.4, 22.1 | 6.0 |
| 16-04-85 | 00:40 | 39.8, 20.6 | 4.7 |
| 16-04-85 | 11:17 | 39.9, 20.1 | 4.4 |
| 16-04-85 | 12:47 | 39.7, 20.8 | 4.6 |
| 16-04-85 | 13:08 | 39.7, 20.7 | 4.2 |
| 16-04-85 | 19:00 | 39.9, 20.1 | 4.4 |
| 11-05-85 | 07:30 | 39.2, 20.6 | 4.6 |
| 12-05-85 | 00:43 | 38.8, 19.8 | 4.5 |
| 21-05-85 | 23:27 | 39.9, 20.5 | 4.6 |
| 13-08-85 | 13:49 | 38.0, 21.4 | 5.1 |
| 31-08-85 | 06:05 | 39.0, 20.4 | 5.5 |
| 31-08-85 | 06:33 | 39.0, 20.4 | 4.3 |
| 17-12-86 | 21:19 | 39.6, 20.1 | 5.6 |
| 09-01-88 | 01:02 | 41.0, 19.7 | 5.6 |
| 26-03-88 | 20:35 | 40.3, 19.6 | 5.5 |
| 24-04-88 | 10:10 | 38.7, 20.2 | 5.0 |
| 09-05-88 | 16:52 | 37.7, 19.8 | 5.0 |
| 18-05-88 | 05:17 | 38.2, 20.2 | 5.9 |
| 22-05-88 | 03:44 | 38.4, 20.4 | 5.5 |
| 02-06-88 | 10:35 | 38.3, 20.4 | 5.0 |
| 06-06-88 | 05:57 | 38.3, 20.4 | 5.0 |
| 22-09-88 | 12:05 | 37.9, 20.9 | 5.1 |
| 30-09-88 | 13:03 | 37.7, 21.3 | 4.9 |
| 16-10-88 | 12:34 | 37.9, 21.0 | 6.0 |
| 08-03-89 | 05:57 | 40.3, 19.1 | 4.9 |
| 07-06-89 | 19:45 | 38.0, 21.6 | 5.2 |
| 20-08-89 | 18:32 | 37.2, 21.1 | 5.9 |
| 24-08-89 | 02:13 | 37.9, 20.1 | 5.7 |
| 31-08-89 | 21:29 | 38.2, 21.8 | 4.8 |
| 29-10-89 | 19:34 | 39.3, 21.2 | 4.2 |
| 29-10-89 | 19:36 | 39.3, 21.1 | 4.5 |

not give an SES at station IOA (almost 2 weeks before, on April 12th, 1985, a series of SES was detected at station IOA, but, for reasons discussed below, it should be correlated with seismic activity which occurred close to that station).

4.1. Procedure for the construction of a selectivity map of a given station

As a general rule, we can state that a trustworthy procedure should be based on earthquakes (or earthquake sequences) that:

(1) happen to be isolated in time;

(2) have appropriate large magnitudes so that the expected SES amplitude should exceed the noise level (which is usually around 0.1 mV for a dipole length of 50 m) by a significant factor (e.g., 4–5).

The SES amplitude depends not only on the resistivities of the dipoles of each station; this gives different values of (appropriate) magnitude thresholds as a function of the epicentral distance, r for different stations. However, as a rough guide, one can rely on the following indicative values: for epicentral distances of the order of a few tens of kilometres, the SES are clearly seen for EQ magnitudes of at least 4.0; when r is around 100 km, the appropriate M_s value should be at least around 5.0–5.5. For even larger epicentral distances (i.e., around 150–200 km), the

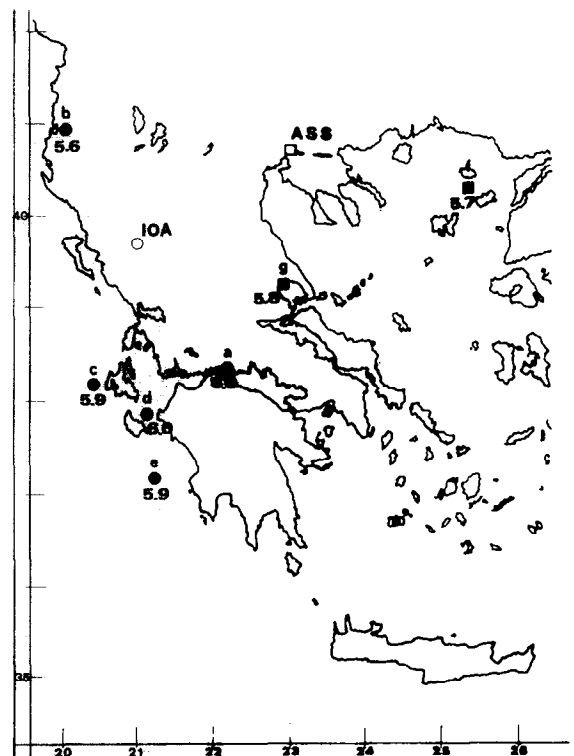


Fig. 3. Map showing the epicenters of a number of earthquakes with $M_s \geq 5.6$ with relatively large epicentral distances from station ASS (\square) and station IOA (\circ). \blacksquare = the epicentres of EQs with SES detected at station ASS; \bullet = those EQs detected at station IOA. a – g = EQs of the following dates (see Tables 1 and 2): a = 11-02-84; b = 09-01-88; c = 18-05-88; d = 16-10-88; e = 20-08-89; f = 10-10-83; and g = 30-04-85.

appropriate magnitude threshold should be close to 6.0.

We clarify again that the above values are no indication of the epicentral distances up to which traces of the SES of an EQ of the aforementioned magnitudes are detectable (Fig. 11); they simply indicate the appropriate limits above which a very clear distinction of SES from the background noise (i.e., with a signal/noise ratio, as mentioned, of at least 4–5) is expected.

The construction of a selectivity map can be attempted after a long period of continuous operation of a station. It should involve the following consecutive steps:

4.1.1. First step: selectivity to earthquakes at large epicentral distances

We selected periods of the order of a few months during which no significant seismic activity was observed in the vicinity of the station; that

is, periods during which EQs with magnitudes of around 4.0 (or larger) occurred within an epicentral distance of the order of about 50 km were excluded. Among the periods selected we restricted ourselves to those that contained earthquakes that were isolated in time (e.g., one EQ during a period of a few months) and with appropriate magnitudes that would warrant a clear SES detection at the station. We then construct a time chart showing these EQs, along with the SES observed at that station (above a certain amplitude) and examine their possible correlation.

As an example Figure 12a shows the time chart of station ASS for continuous 3 month period: April 1st 1985, to June 30th, 1985. Only one SES was collected with an amplitude larger than 0.5 mV on either of the two perpendicular short dipoles ($L = 70$ m); it was recorded on April 25th, on all the dipoles of the station but the $\Delta V/L$ value on the E–W component was appre-

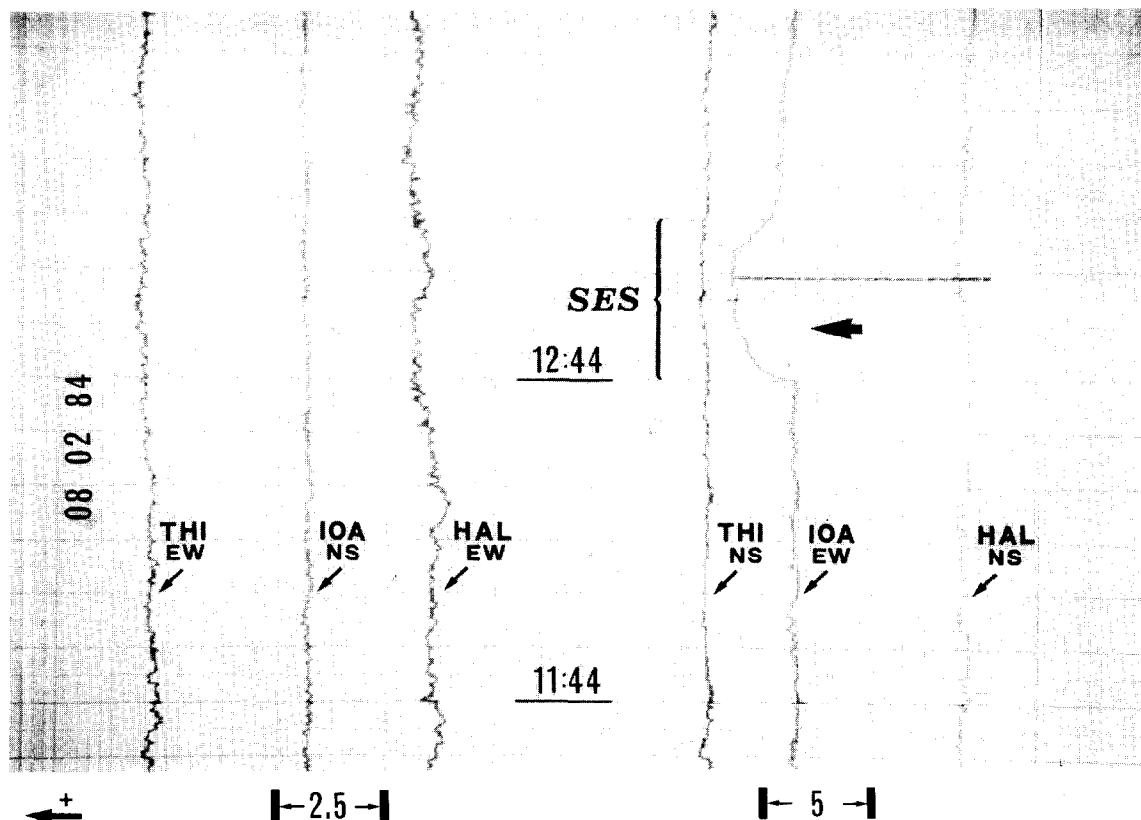
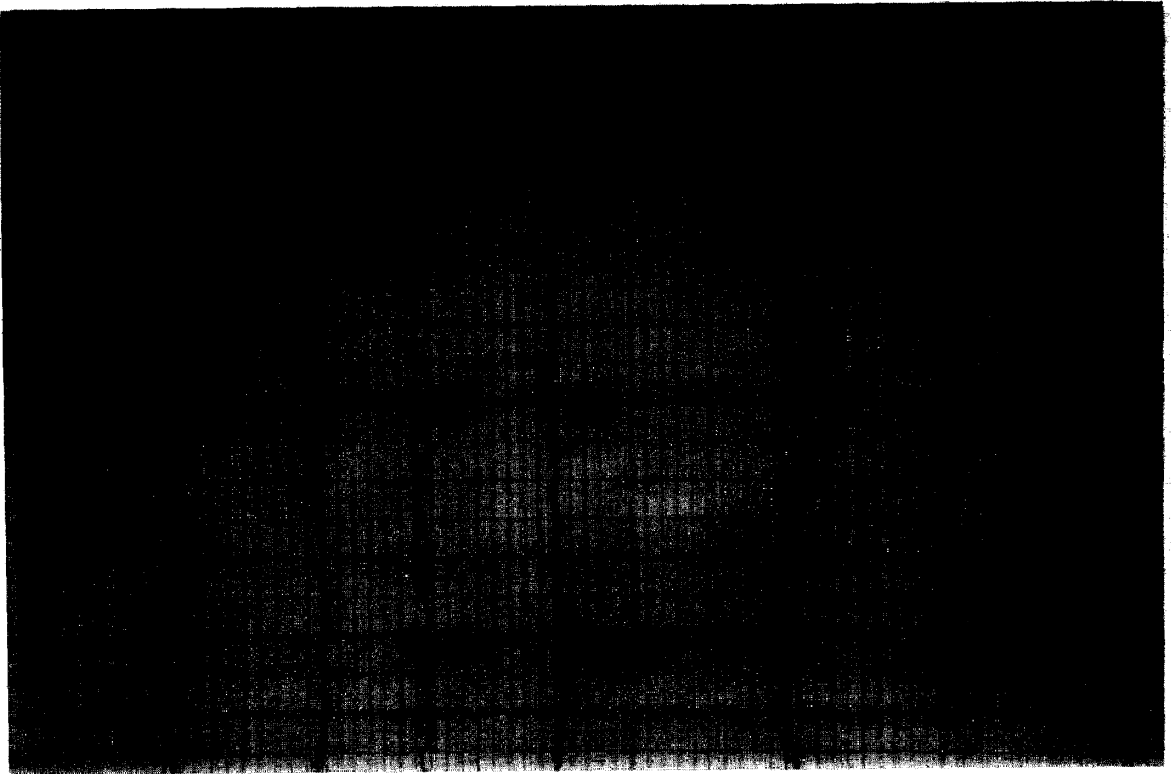
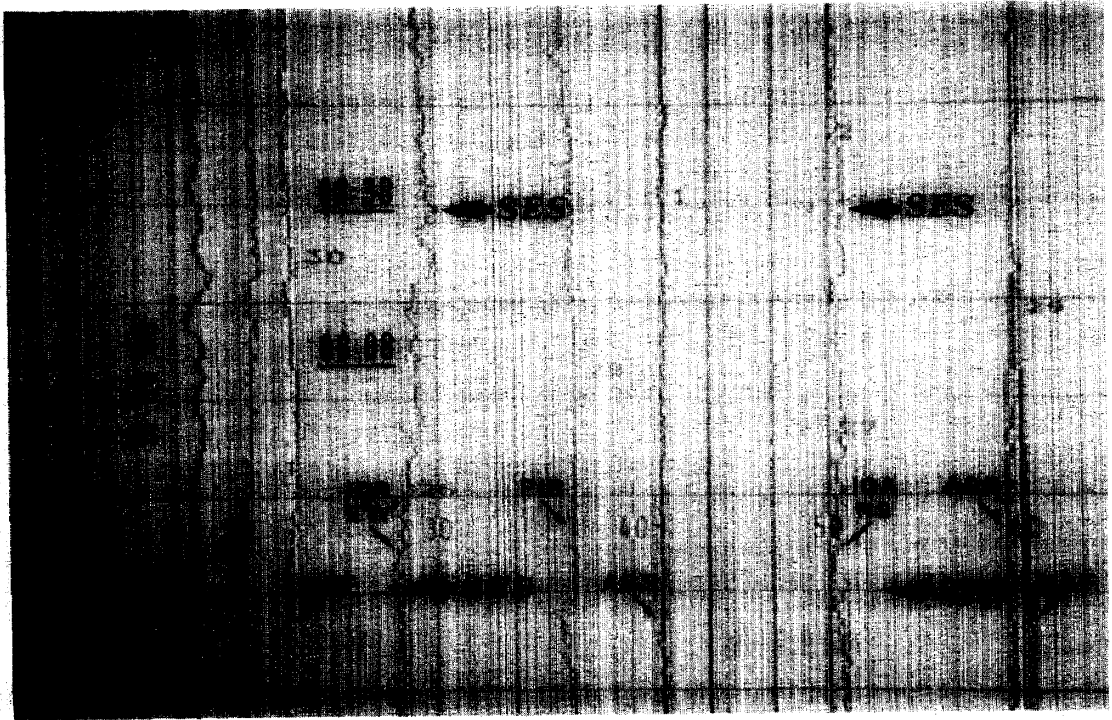


Fig. 4. SES detected on February 8th, 1984, on the short E–W dipole ($L = 47.5$ m) at station IOA. The corresponding earthquake ($M_s = 6.0$) occurred on February 11th, 1984, with an epicenter at 38.4°N , 22.1°E (EQ *a*, Fig. 3). For the help of the reader we clarify that the configuration of the eight dipoles installed at station IOA is depicted in fig. 2 of Varotsos et al. (1993, this issue).



← 12.5 → ← 25 → ← 5 → ← 62.5 → ← +



+ → ← 5 → ← 5 →

ciably larger than that of the N-S component (fig. 4, Paper I). This SES was followed by a 5.8 EQ that occurred on April 30th, 1985, with an epicentre at 39.3°N, 22.9°E, at a distance around 130 km from station ASS. This EQ is well isolated in time and space because no other EQ occurred during this 3-month period with the following magnitude thresholds: $M > 4$ with $r < 50$ km; $M > 4.5$ with $50 < r < 100$ km; $M > 5$ with $100 < r < 300$ km or $M > 5.5$ at distances up to 400–500 km. Therefore, Fig. 12a shows that the single SES can only be correlated with the single EQ. The same investigation should be repeated for other periods in order to confirm that station ASS is selective to the area labelled *b* in Fig. 2. It should be remembered that all EQs from area *b* should give SES at station ASS with the same polarity and with linear plots of $\log \Delta V/L$ versus M for each component with a slope around 0.34–0.37.

4.1.2. Second step: selectivity to earthquakes at relatively small distances

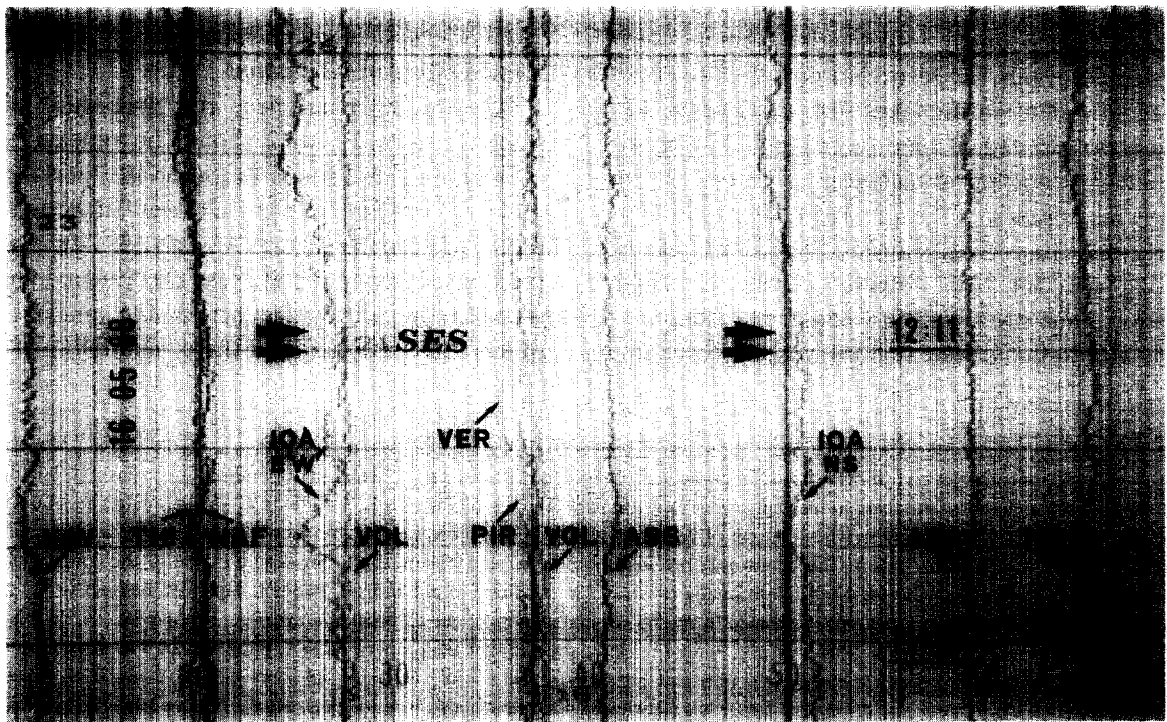
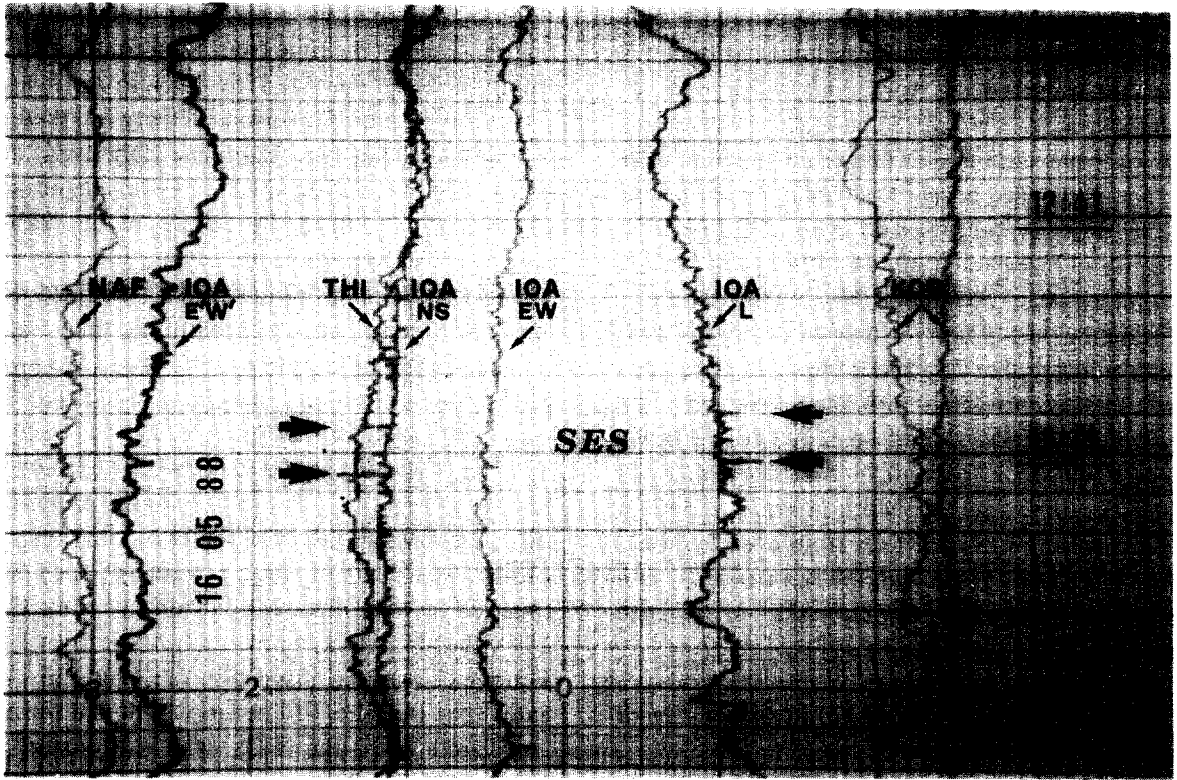
We selected periods of at least of a few months during which no earthquakes occurred, at distances of around 100 km or more which had magnitudes that would provide a clear SES record at the station under investigation. Among such selected periods, we restricted ourselves to those that included earthquakes (or earthquake sequences) isolated in time (e.g. one EQ in a few months) at epicentral distances of around 50 km with magnitudes of 4.0 or larger. We then constructed a time chart showing these earthquakes, along with the SES observed during the same period, thus investigating whether the station is selective to the seismic regions lying in its vicinity.

As an example, we refer again to station ASS. Figure 13 shows the time chart for a continuous $2\frac{1}{2}$ month period (February 15th, 1984, to April 30th, 1984), during which a seismic activity (marked *b*) lasting only 1 day (i.e., February 19th, 1984) and comprising four earthquakes with magnitudes larger than 4.0, all in the vicinity of the station (Table 1) was reported. Note that, at larger epicentral distances no significant EQ occurred during that period with a magnitude that would warrant a clear SES; that is, no EQ occurred with $M \geq 4.5$ at $r \leq 100$ km, with $4.5 < M < 5.0$ at $100 < r < 200$, with $5.0 < M < 5.5$ at $200 < r < 300$ or with $5.5 < M < 6.0$ at $300 < r < 500$; etc. In Figure 13 we insert the SES that had an amplitude $\Delta V > 0.5$ mV on either of the two perpendicular short ($L = 70$ m) dipoles; a series of such SES (marked *a*) were recorded only on February 17th, 1984, that is 2 days before the seismic activity of February 19th. An inspection of Figure 13 indicates that the SES of February 17th can only be correlated with the EQs which occurred on February 19th. This result suggests that station ASS is selective to a seismic area lying in its vicinity (Fig. 2).

4.1.3. Third step: combination of the results obtained for various stations

As already mentioned, the procedure indicated in steps 1 and 2 should be repeated for each station at various (appropriate) periods in order to confirm the correlations suggested by figures similar to Figures 12 and 13. After completing this study for at least two (independent) stations, the self-consistency of the analysis requires the examination of the compatibility of the

Fig. 5. (a) SES detected at IOA on May 15th, 1988, by both component dipole arrays. The corresponding directions and lengths of the dipoles are as follows (the scale in the figure is in millivolts): E-W, $L = 47.5$ m; N-S, $L = 48$ m; E'-W', $L = 181$ m. The dipole labelled IOA has a NNE direction, with a length of 2.5 km; the sites of its two electrodes are shown in fig. 25, Paper I and in fig. 2 of Varotsos et al. (1993, this issue). The apparently reversed polarity of the SES on the latter dipole is due to the connections of this dipole to the amplifier, having been intentionally reversed, as explained in appendix 2, Paper I. This SES belongs to the same SES series as those of Fig. 6; they were followed by strong seismic activity in the Cephallonia area (i.e. around 38.2°N, 20.2°E) the largest EQ occurred on May 18th, 1988, with $M_s = 5.9$ (Table 2, and the first telegram of table 1, Paper I). (b) The same SES as in (a) but recorded on a dot point recorder at a different pair of dipoles: E'-W' with $L = 48$ m, N-S with $L = 100$ m. Due to a sampling rate of 1 dot/8 sec the deviations appear as a series of dots (this is also true for Figs. 6b, 8b, 9b and 10b). The polarity of this dot-point recorder is opposite to that in (a) and hence the SES in both have the same polarity. A combination of (a) and (b) leads to a verification of the law $\Delta V/L = \text{constant}$ for the parallel short dipoles of various lengths.



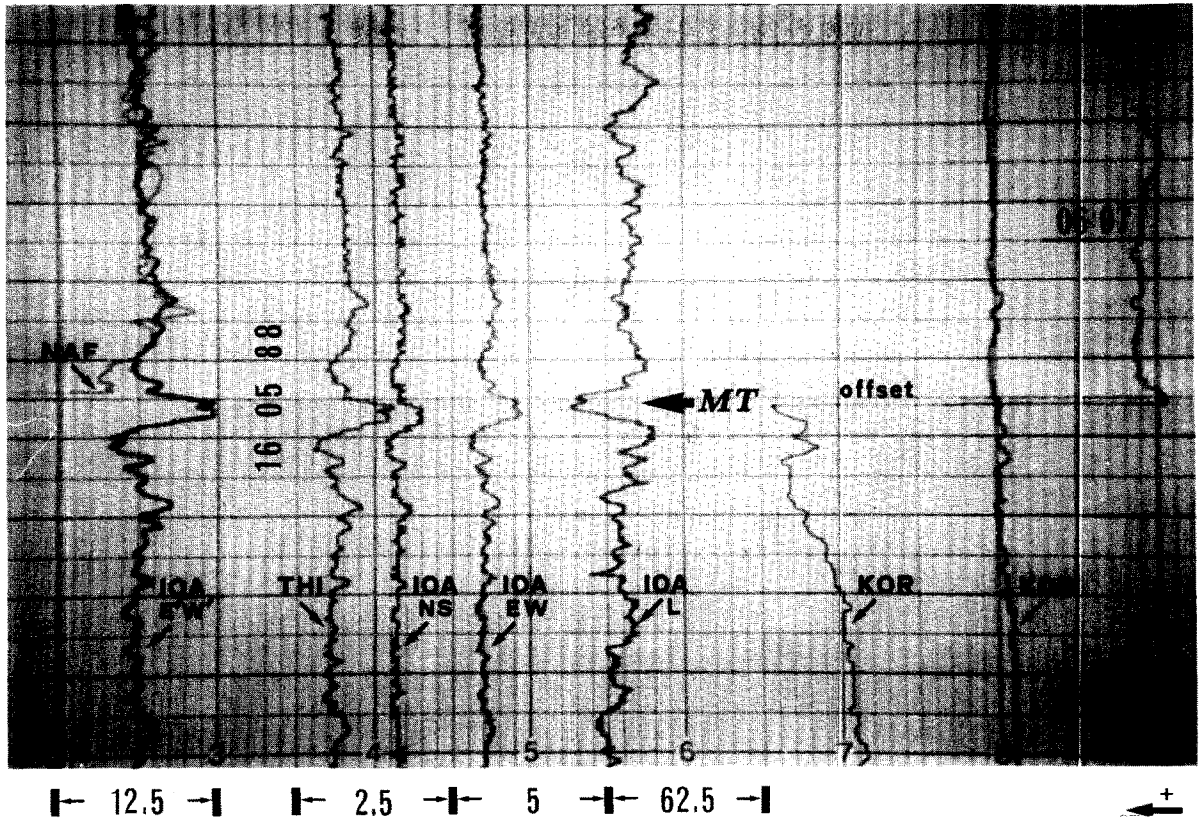


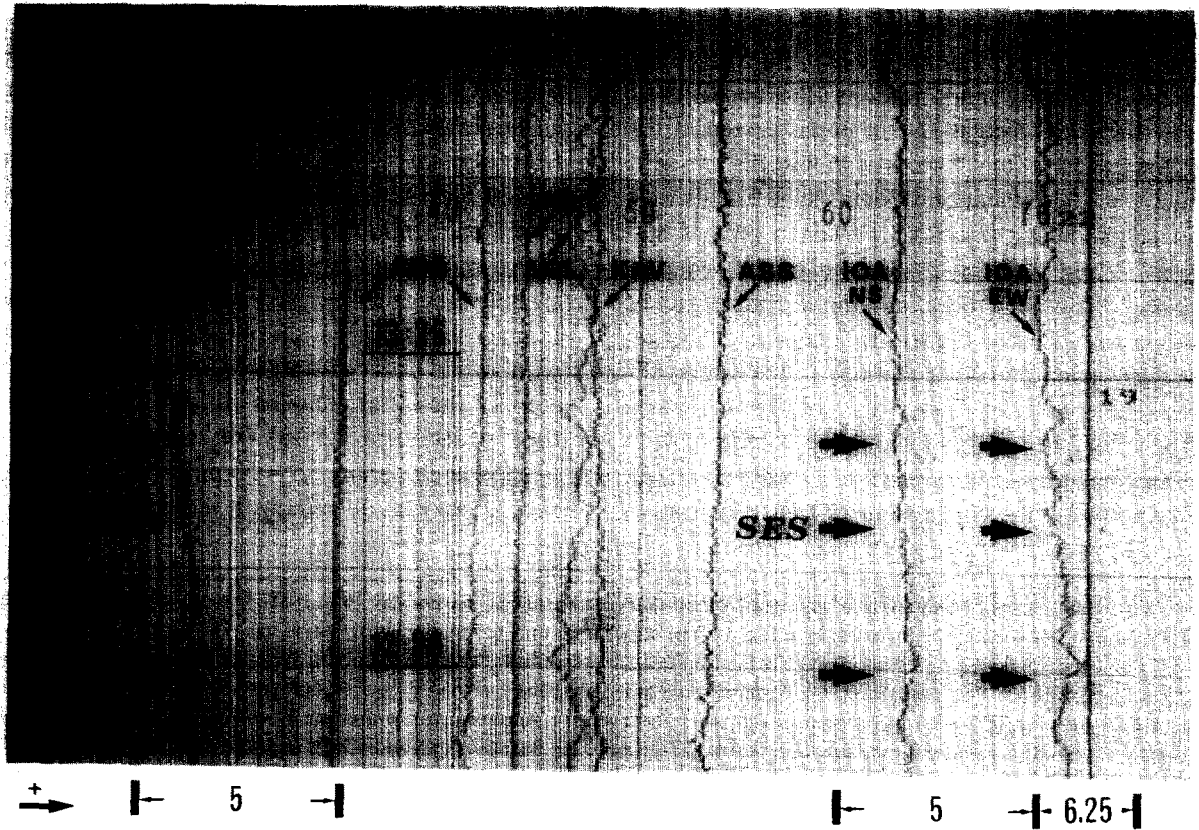
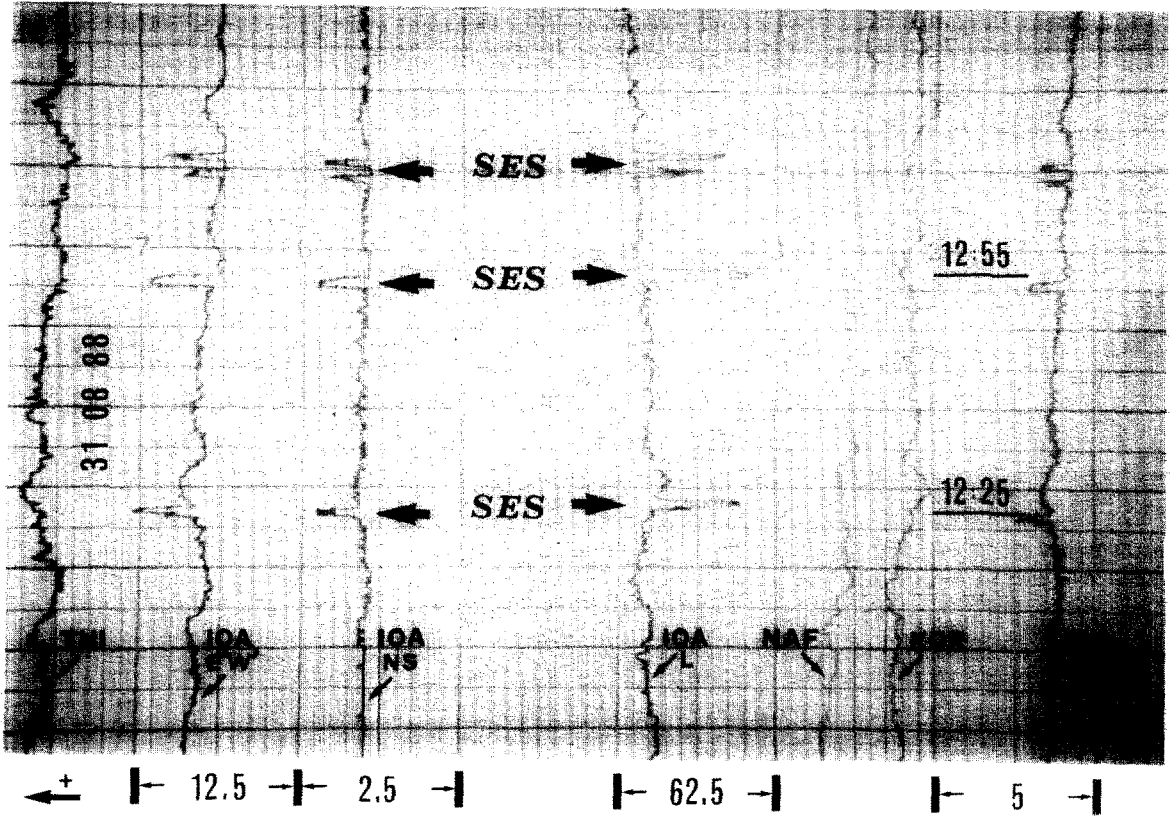
Fig. 7. Magnetotelluric disturbances detected at station IOA on the same dipoles as in Figs. 5a and 6a.

conclusions drawn independently for these two stations. Among other reasons, the necessity of this further investigation can be visualized in the following way: step 1 deals with the distant seismicity of a given station whereas step 2 deals with its neighbouring seismicity. When a pair of stations, i and j , lie at a distance of 150 km, for example, a seismic area, a , lying in the vicinity of the station i could constitute a source of distant seismicity for the other station, j . Therefore, for the sake of self-consistency the conclusions drawn from step 2 for station i should be compared with those of step 1 for in station j and vice versa. Furthermore, the conclusions of step 1 for station

i should also be compared to those of step 1 for station j in order to examine whether strong earthquakes lying at more or less equal distances from stations i and j , give either simultaneous SES at both stations or SES that can be collected at the one station but not at the other.

As an example, we apply step 3 to the pair of stations ASS and IOA. In Figure 14 we reproduce Figure 12a of station ASS obtained in step 1 along with a time chart of station IOA (corresponding to step 2); the latter contains all SES with an amplitude of at least 0.5 mV on either of the two perpendicular short ($L = 50$ m) dipoles of station IOA, along with all EQs with the following magni-

Fig. 6. (a) Series of SES (only the two largest indicated) detected at station IOA on May 16th, 1988. The corresponding directions and lengths of the dipoles are the same as in Fig. 5a. The scales refer only to the dipoles of station IOA. The series of SES shown in Figs. 5 and 6 was followed by seismic activity in the Cephallonia area, which began on May 18th, 1988 (see Table 2) and included an EQ of magnitude 5.9. For comparison, Fig. 7 shows some MT disturbances recorded on the same day at the same dipoles. (b) The same SES series as in (a) but recorded on a dot point recorder at a different pair of dipoles: E'-W' with $L = 48$ m, N-S with $L = 100$ m. The SES polarity is the same with that in (a) (because the recorders in a and b have opposite polarities, as explained in Fig. 5). The scales refer only to the dipoles of station IOA. A verification of the rule: $\Delta V/L = \text{constant}$ can be easily obtained when comparing the parallel short dipoles of (a) and (b).



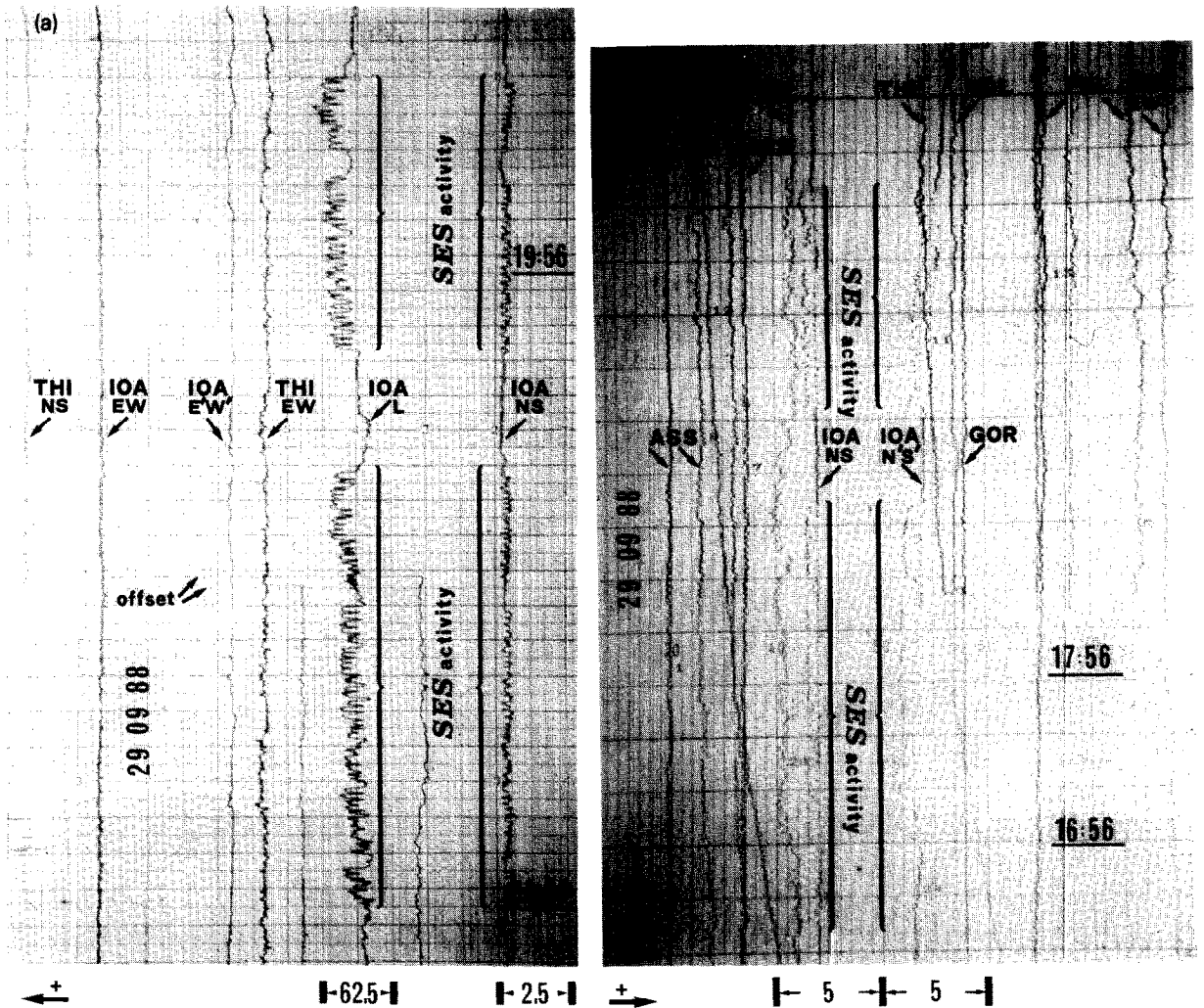


Fig. 9. (a) SES activity detected on September 29, 1988 at station IOA. This is the second of the three SES sequences that preceded the Killini-Vartholomio destructive earthquakes mentioned in Fig. 8a. The dipoles are the same as in Figs. 5a, 6a and 8a, but the SES depicted in Figs. 8a and 9a (see appendix 2, Paper I), have a different polarity. This difference was attributed to a slight displacement of the epicentre (in comparison to the EQ of September 22nd, 1988), as mentioned in telegram 11, table 1, Paper I. (b) The same SES activity detected at station IOA as in (a) and recorded on a dot point recorder. The dipoles are the same as in Fig. 8b. The polarities of the SES of (a) and (b) are the same.

tudes: $M_s \geq 4.2$ for epicentral distances less than 100 km and EQ larger than 5.0 for $100 < r < 300$ km.

An inspection of these two time charts leads to the following considerations about their compatibility: On April 12th, 1985, a series of SES, all

Fig. 8. (a) SES activity detected on August 31st, 1988, at station IOA. The dipoles are the same as in Figs. 5a and 6a. This is the first of the three SES sequences that preceded the Killini-Vartholomio destructive earthquakes of September–October 1988 (Table 2, and appendix 2, Paper I) and were publically announced. It corresponds to the telegram shown in fig. 21 of Paper I. (b) The same SES activity detected at station IOA as in (a) but recorded on a dot point recorder. The dipoles: E–W with $L = 100$ m; N–S with $L = 100$ m; N'–S' with $L = 184$ m, have no common electrodes with those in (a). In addition to the seven dipoles shown an eighth dipole (E–W direction), with $L = 48$ m was operating; it also collected the SES but its trace lies outside the confines of the photograph. The scale is the same for all IOA traces. These SES have the same polarity as those recorded on the short dipoles of (a).

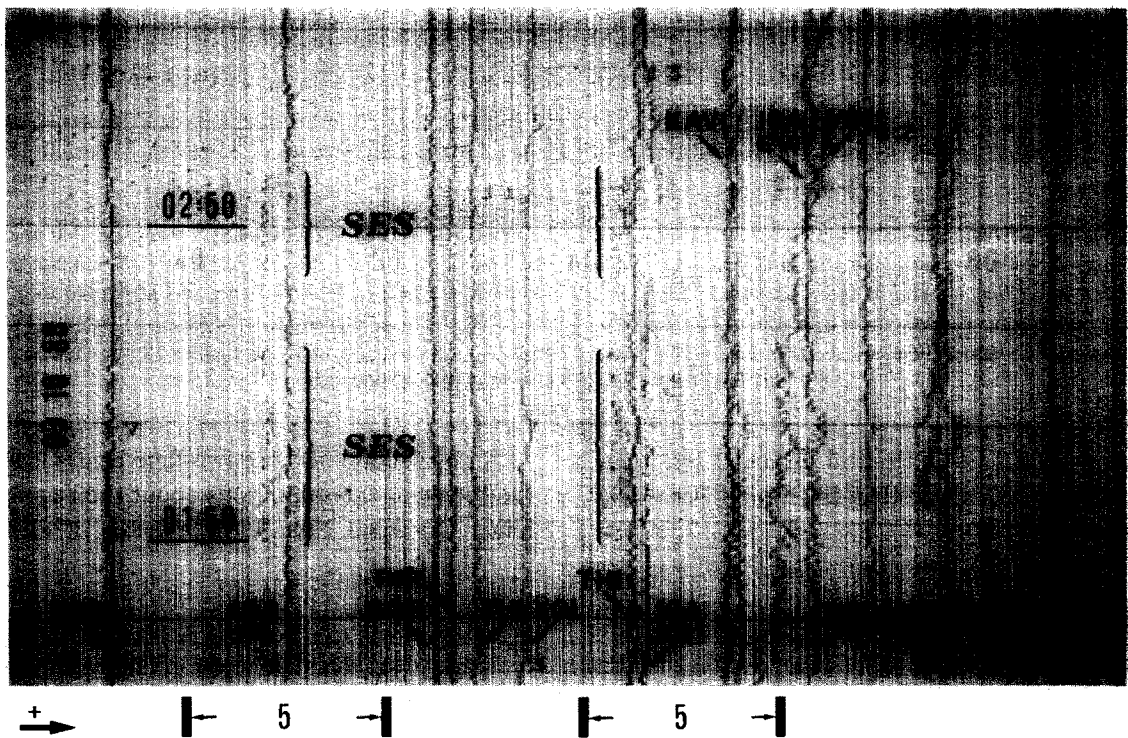
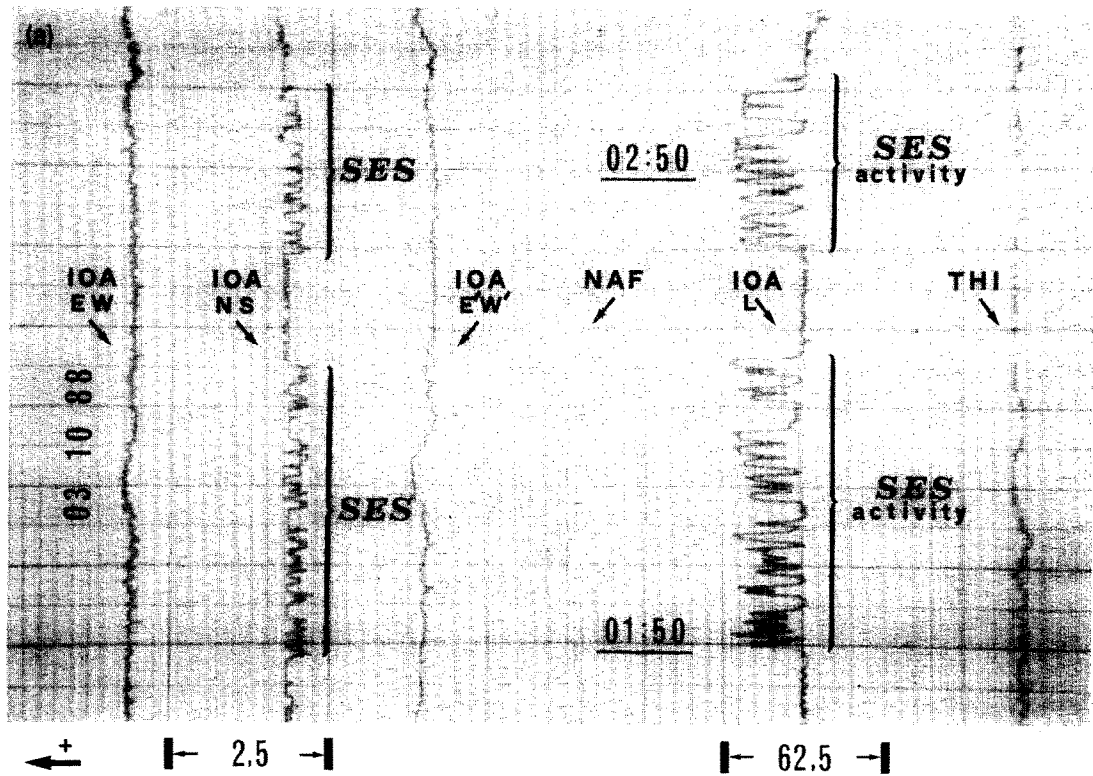


Fig. 10. (a) SES activity detected on October 3rd, 1988, at station IOA. This is the third SES sequence that preceded the Killini-Vartholomio destructive earthquakes mentioned in Figs. 8a and 9a. It corresponds to the telegram 12, table 1, Paper I. The dipoles are the same as in Figs. 5a, 6a, 8a and 9a. (b) The same SES activity detected at station IOA as in (a) but recorded on a dot point recorder. The dipoles are exactly the same as those depicted in Fig. 9b (except for the dipole labelled with E'-W', which has a length of 100 m and was also mentioned in the caption of Fig. 8b).

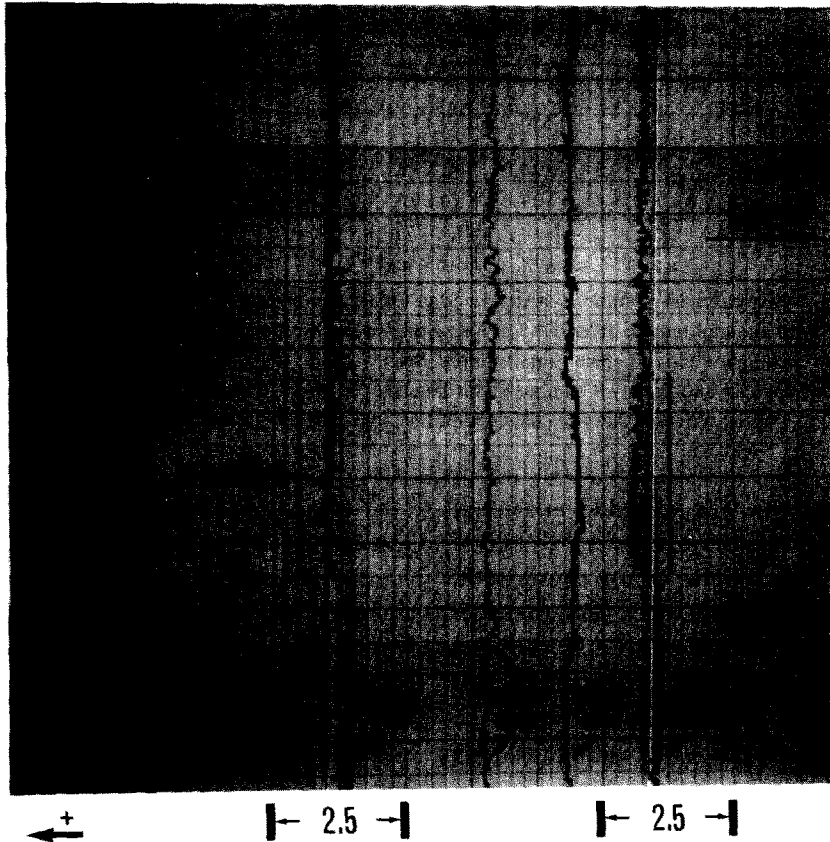


Fig. 11. SES detected at both perpendicular short ($L = 70$ m) dipoles of station ASS on October 7th, 1983. It was followed by a $M_s = 5.7$ EQ that occurred on October 10th, 1983, with an epicenter at 40.9°N , 25.5°E (in area *a* of the selectivity map of station ASS, Fig. 2).

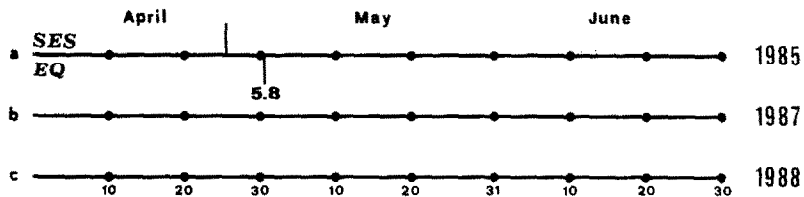


Fig. 12. Time chart (a) of station ASS for a 3 month period: April 1st, 1985, to June 30th, 1985. It depicts all SES with an amplitude larger than 0.5 mV on either of the two perpendicular short dipoles ($L = 70$ m). Only the earthquakes that would warrant a clear SES are considered (see text): $M \geq 4$ with $r \leq 50$ km; $M \geq 4.5$ with $50 < r \leq 100$ km; $M \geq 5$ with $100 < r \leq 300$ km; $M \geq 5.5$ with $400 < r < 500$ km. Time charts (b) and (c) made for the same months of 1987 and 1988 show that the SES shown in (a) are rare.

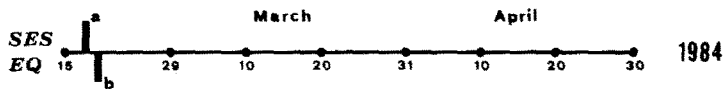


Fig. 13. Time chart of station ASS for the period February 15th, 1984, to April 30th, 1984. It depicts all SES with an amplitude larger than 0.5 mV on either of the two perpendicular short dipoles ($L = 70$ m), along with all EQ that would warrant a clear SES detection ($M \geq 4.5$ at $r \leq 100$ km; $M > 4.5$ at $100 < r < 200$; $M \geq 5.0$ M at $200 < r < 300$; $M \geq 5.5$ at $300 < r < 500$. *a* = SES on February 15th; *b* = EQ on February 19th.

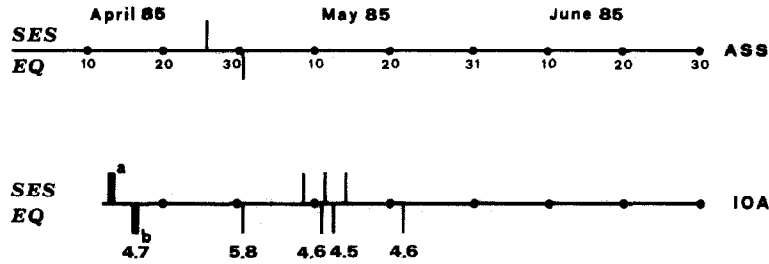


Fig. 14. Reproduction of the time chart of station ASS described in Fig. 12a, along with a simultaneous time chart of station IOA; the latter includes all SES with an amplitude of at least 0.5 mV on either of the two perpendicular short ($L = 48$ m) dipoles, along with all EQs with the following magnitudes and epicentral distances: $M_s > 4.2$ for $r < 100$ km and $M_s \geq 5.0$ for $100 < r < 300$ km. $a =$ a number of SES shown in Figs. 15 and 16; $b =$ a number of earthquakes ($M_s \leq 4.7$) with epicentres listed in Table 2. The parameters of the other earthquakes included in this time chart are also given in Table 2.

with the same polarity was recorded at station IOA (Fig. 15). This was followed by a number of EQs with magnitudes up to 4.7 on April 16th, 1985 (Table 2) lying at distances less than (or around) 50 km from that station. Before claiming any correlation we state that, in principle, this SES series of April 12th, 1985, could either be correlated with the neighbouring seismic activity

of April, 16th or with the 5.8 event of April 30th, lying at a distance of around 200 km from station IOA. The latter possibility however can be excluded for various reasons based on the physical properties of SES discussed in Paper I. One of these properties states that: "SES of earthquakes of comparable magnitude coming from the same seismic area, are recorded on the same station

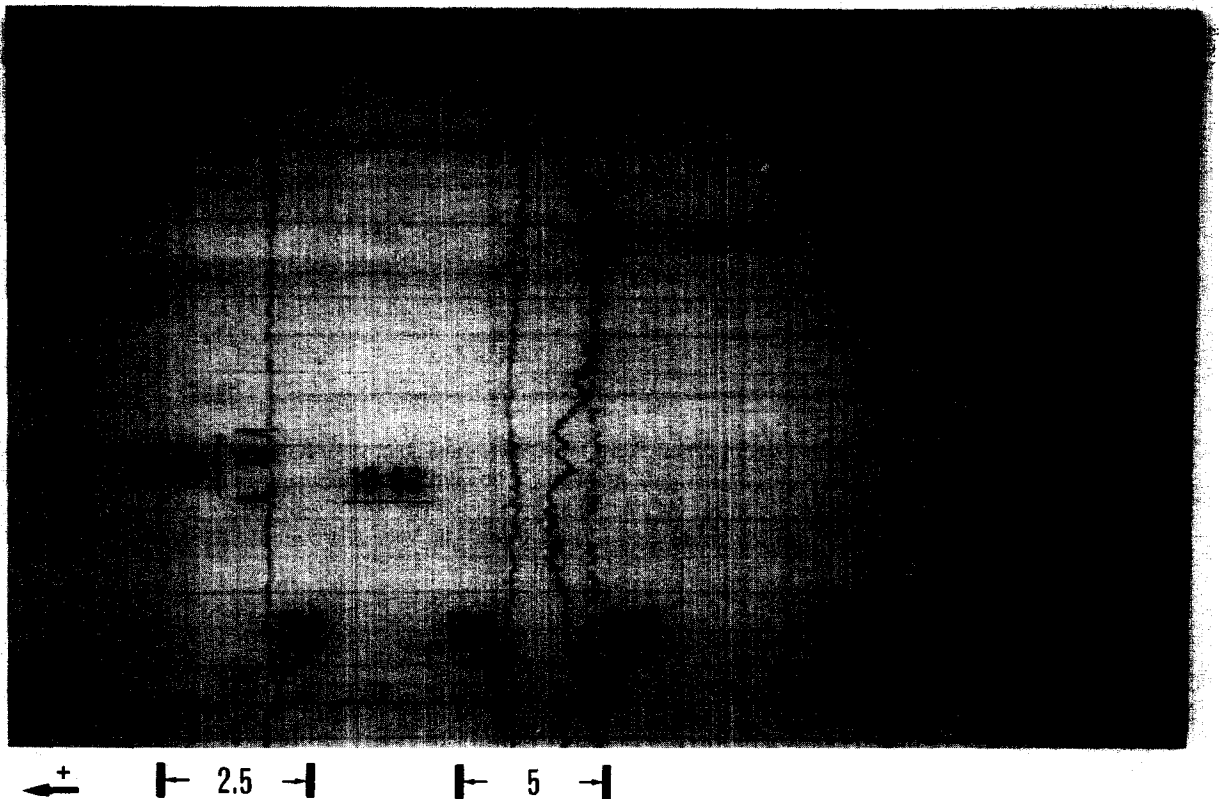


Fig. 15. A sequence of four SES detected at the N-S short ($L = 47.5$ m) dipole of station IOA on April 12th, 1985. It was followed by an earthquake sequence on April 16th, 1985 (Table 2), with epicentral distances of less than (or around) 50 km.

with the same polarity and the same amplitude". By recalling this property we draw the attention to the following fact: An SES with practically the same amplitude, the same polarity and the same $\Delta V_{EW}/\Delta V_{NS}$ ($L = \text{constant}$) ratio was also recorded at station IOA on May 14th, 1985 (Fig. 16) but was not followed by an event from the seismic area 39.3°N , 22.9°E where the 5.8 EQ of April 30th, 1985 had occurred. However, this SES was followed by a $M_s = 4.6$ EQ on May 21st, 1985, from the same seismic area that also became active on April 16th; therefore a self-consistent analysis indicates that the SES activity of April 12th has to be correlated with the neighbouring EQs of April 16th (for comparison, see also Figures 17 and 18, which refer to SES from a neighbouring seismicity but from a different seismic area). In view of this result, an inspection of Figure 14 reveals that the only SES that can be correlated to the 5.8 event of April 30th is actually that observed at station ASS on April 25th; it

also means that the seismic area labelled *b* in Figure 2 (around 39.3°N , 22.9°E) does not give SES that are simultaneously recorded at IOA and ASS. This fact is also confirmed for other seismic areas, thus concluding, as already mentioned, that the selectivity maps of IOA and ASS do not have any common area. In addition, it means that there must be a physical "boundary" lying between IOA and ASS that does not allow the "SES communication" between these two stations. In Tables 1 and 2 earthquakes or earthquake sequences that give SES either recorded at station IOA (Table 2) or at station ASS (Table 1) are listed. These lists are *indicative* of the extent of the selectivity maps of the corresponding stations (Fig. 2).

5. Other types of electrical precursors observed in Greece

Figure 19 shows schematically that, beyond the SES, two other types of electrical precursors have

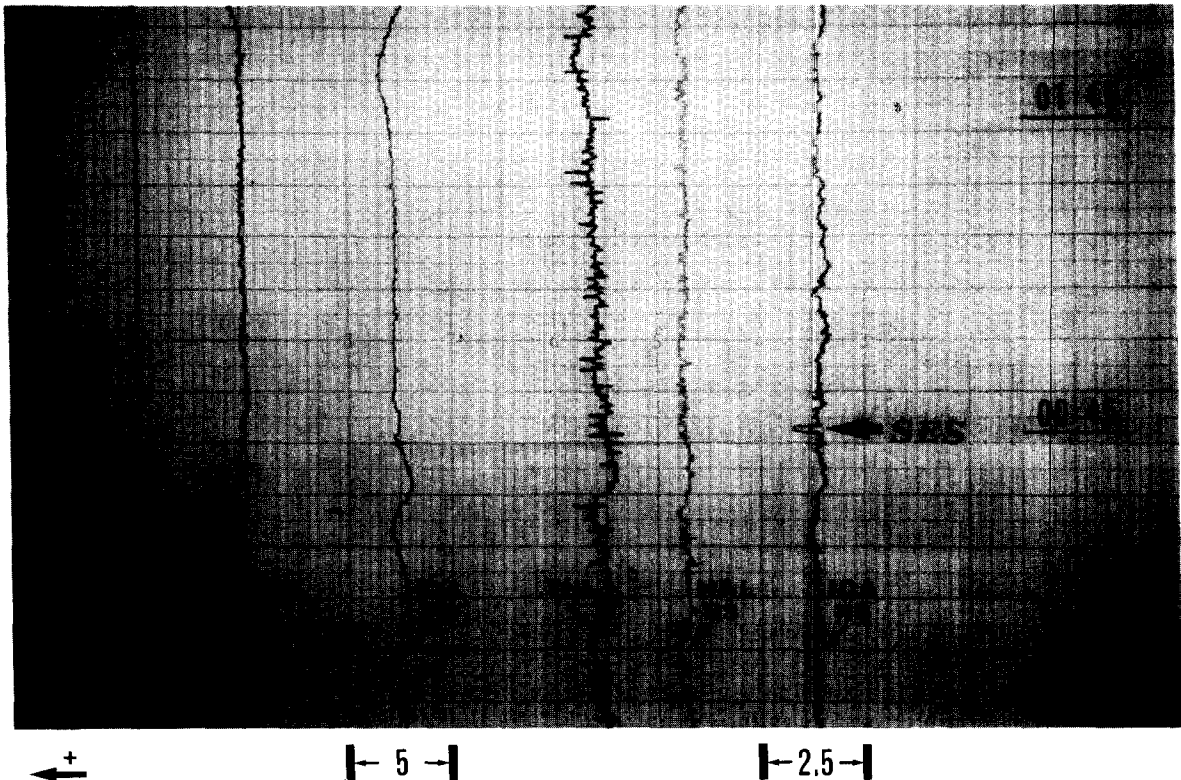


Fig. 16. SES detected on May 14th, 1985, at the short ($L = 47.5$ m) N-S dipole of station IOA. It has the same polarity as the SES in Fig. 15 and was followed by a 4.6 EQ with an epicenter at 39.9°N , 20.5°E , that is, from the same seismic area that emitted the SES sequence shown in Fig. 15.

been observed in Greece. One of them is a very slow variation (i.e. it has a duration of the order of a couple of weeks) and precedes the appearance of the SES by a few weeks; the other one is very short (i.e. with a duration of some milliseconds) and is detected immediately before the occurrence of an EQ. Their basic features are summarized below.

5.1. Gradual variation in the electric field of the earth (GVEF)

This bay-like anomaly is observed for events with magnitude 5.5 or larger. It appears a couple

of weeks (or more) before an EQ and reaches (at the time of the maximum deviation) an amplitude of one order of magnitude greater than the SES. From consideration of the entire 8 yr of continuous monitoring, we can state the following:

(1) A GVEF has only been observed in a few cases; whenever it was observed it was followed by significant seismic activity, that is, by an EQ of $M_s \geq 5.5$. As an example we refer to a GVEF recorded at station PIR; it started the last week of April 1987, and was followed by two significant shocks of $M_s = 5.6$ on May 29th, 1987 and June 10th, 1987, respectively.

(2) Cases have been observed where a station very close (i.e., up to a few tens of kilometers) to

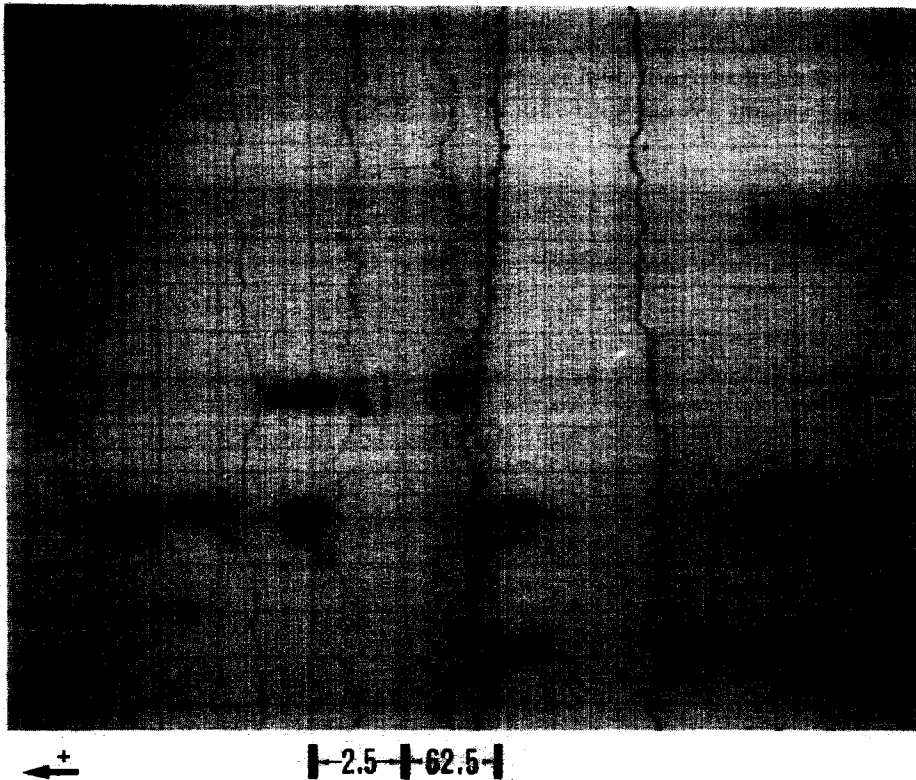


Fig. 17. An SES sequence detected on October 18th, 1989, at the N-S short ($L = 47.5$ m) dipole of station 10A. It was also recorded on the long ($L = 2.5$ km) dipole (labelled 10A) that is almost directed in NNE, direction; the sites of its electrodes are depicted in fig. 25, Paper I. The apparently reversed polarity of the SES on the 10A trace is due to the connections of the dipole to the amplifier being intentionally reversed (as described in appendix 2, Paper I). The sequence was followed by 11 earthquakes that occurred almost within 4 h (i.e., from 19:29 to 23:50 GMT) on October 29th, 1989, with epicentres lying in the area $38.9\text{--}39.3^\circ\text{N}$; $21.1\text{--}21.2^\circ\text{E}$ and with M_s values between 3.4 and 4.5. Two of these EQs had magnitudes of 4.2 and 4.5 (Table 2, and telegram 22 of table 4, Paper I) and epicentral distances of around 50 km to the east-southeast of station 10A. Note that the SES polarity of the N-S dipole of this figure is opposite to those shown in Figs. 15 and 16, which corresponded to a sequence of earthquakes with comparable magnitudes but with epicentres a few tens of kilometres to the north (and northwest) of 10A.

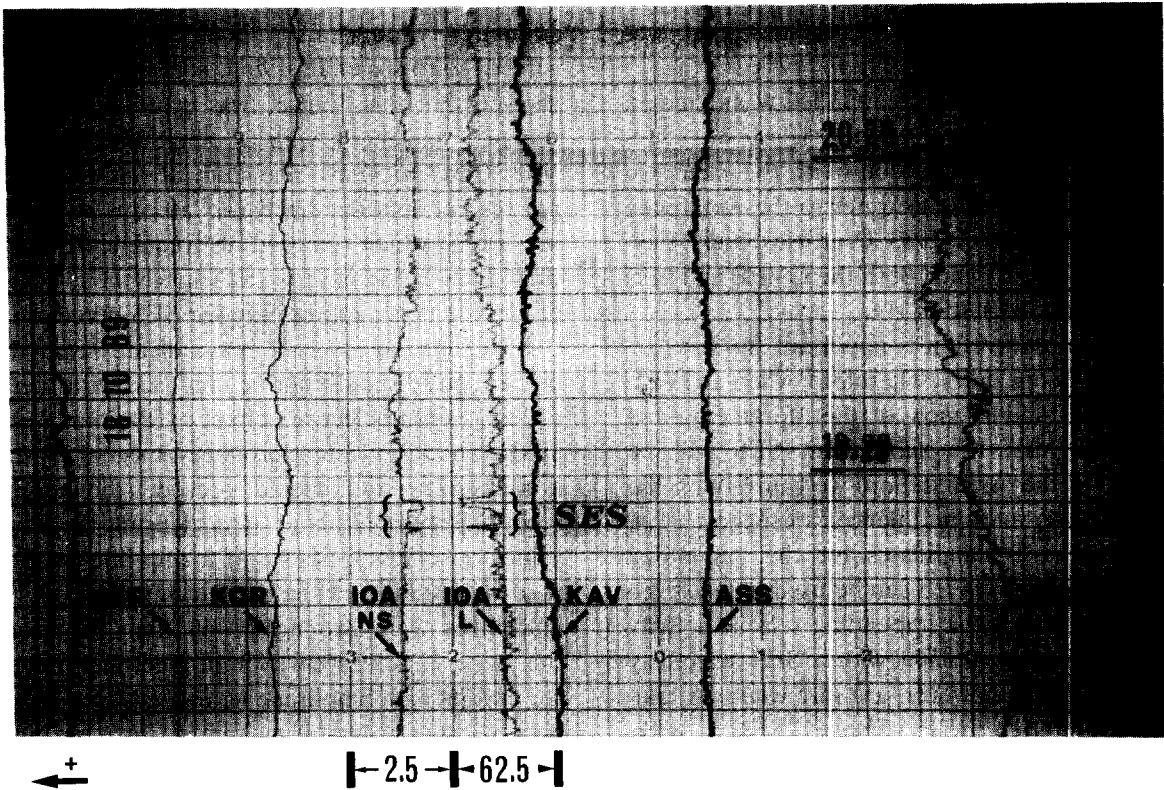


Fig. 18. SES detected at station IOA almost 8 h after the SES of the previous figure and belonging to the same sequence described in Fig. 17.

the epicentral zone did not detect a GVEF. Two characteristic examples are:

(a) The destructive seismic sequence of Killini-Vartholomio ($M_s = 6.0$) in September–October, 1988; station PIR did not record any GVEF although it was only about 30 km from the epicentre of the main shock.

(b) The Kalamata destructive EQ, with $M_s = 6.4$, on September 13th, 1986; station KAL (see

fig. 1, Varotsos and Alexopoulos, 1984a) did not show any unusual variation, although it was only 20–30 km from the epicentral zone.

It should be remembered that, in both examples, clear SES were recorded, at more distant stations; that is, at distances of around 200 km. Thus Killini-Vartholomio seismic activity was preceded by SES recorded at station IOA (see Figs. 8–10), while the SES of the Kalamata EQ were

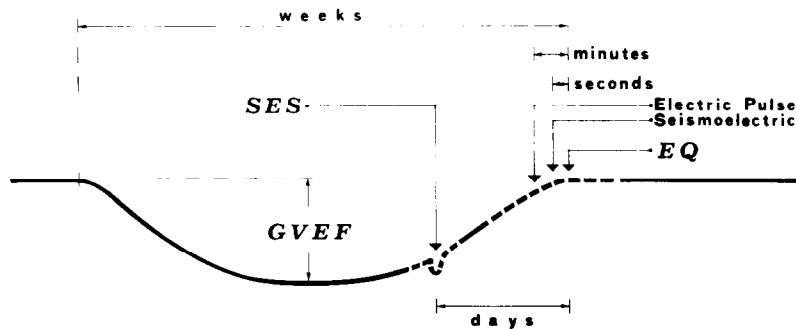


Fig. 19. Schematic representation of the time sequence of the three types of electrical precursors (GVEF, SES and electric pulse) that have been observed in Greece. Not to scales (for the exact values see the text).

collected at station KER (Varotsos and Alexopoulos, 1987).

(3) In rare cases where a GVEF was detected it was *always* followed by, at least, one SES recorded at the same station (with the same polarity). As an example, we refer to the Kefallonia seismic sequence of 1983 (Varotsos and Alexopoulos, 1984a, b) when both the GVEF and SES were recorded at station PIR.

This last observation is important for the prediction of an epicentre. Therefore, when a GVEF is observed (and in view of the aforementioned expectation that the subsequent SES will be recorded at the same station) we can rely on the SES selectivity maps and hence can suggest a few seismic areas as candidates for the impending EQ. Therefore, a GVEF can be used to guess the epicentral area of the impending seismic activity only when it is combined with a SES selectivity map. Such cases, however, are rare when we take into consideration the fact that a GVEF is rarely observed. For example, among the 32 telegrams (predictions) issued during the period 1987–1989, only in one case (the first telegram of table 2, Paper I) was a GVEF observed.

(4) The rare appearance of GVEF in the 8 yr of data collected in Greece does not allow any statement on any correlation between GVEF amplitude and EQ magnitude. Concerning the distance up to which GVEF can be observed, we confirm that although our data include events with M_s up to 7, GVEF were detected only up to distances of 150 km.

5.2. Short duration electric signal before an EQ

During the aftershock period of the 6.5 event that occurred on February 24th, 1981, close to station KOR a 3 month monitoring was carried out using a Carry 401 vibrating reed electrometer. The measurements were made with electric dipoles about 50 m in length at five different sites with epicentral distances up to 60 km from the active zone. In order to achieve a simultaneous on-site observation of the electric and seismic data, a seismograph was also installed at each measuring site. Hundreds of cases were observed in which, 1–4 min before the initiation of the

seismic recording, an “electric pulse” was observed (Varotsos et al., 1981). A preliminary study showed that this “pulse” was up to several milliseconds in length, with an amplitude of a few Volts (for $L = 50$ m). The study of this effect was not further continued because later on we had to use filters, which removed all frequencies higher than a few Hertz in order to achieve the low level of electric noise appropriate for SES detection.

The time lag of 1–4 min indicates that this electric pulse should not be confused with the so called “seismoelectric effect” (Parkhomenko, 1981). The latter effect produces a signal that, at a measuring site, should precede the seismic recording by only about 10 sec; using the usual values seismic velocities and taking into account that the distances of the measuring sites from the epicentres were around 40–60 km. Therefore, this pulse is a different type of electrical precursor and its high amplitude (it exceeds that of the SES by three orders of magnitude, or more) may indicate that, immediately before the rupture, intense “high frequency” disturbances are emitted from the focal area. This observation is in agreement with recent theoretical aspects of Gershenzon and Gokhberg (pers. commun., 1990). Due to the restricted amount of data, no attempt was made to examine whether the parameters of this short duration signal are correlated with the EQ magnitude and/or the epicentral distance.

Summarizing the three types of electrical precursors observed in Greece (GVEF, SES and short duration pulse), we can say that, according to current knowledge, only SES can be used for the determination of the epicentre and magnitude of an impending earthquake.

6. Theoretical models to explain SES generation

It is far from the scope of this paper to review all the models that have been proposed in order to explain the appearance of the various electrical precursors detected to date. We restrict ourselves only to those models that have been recently suggested for the explanation of SES generation. The possible physical processes involved in these models can be classified into:

(1) *Electrokinetic effects*: There are two basic philosophies in this direction: the first approach (Morgan, 1990) considers electrokinetic phenomena in the preparation zone that produce electric field changes at the earth's surface. The second approach (Dobrovolsky et al., 1989; Gershenzon et al., 1990) considers that the state of stress and strain extends to distant points and that, under appropriate conditions, electrokinetic phenomena are produced close to the measuring site, thus giving rise to measurable, transient variations in the potential difference between neighbouring "points" with different electrophysical properties.

(2) *Piezo-stimulated currents*: This model suggests stress-induced (re)orientation of electric dipoles formed by point defects (e.g. impurity–vacancy or impurity–interstitial ion) at the preparation zone. When the stress reaches a critical value (σ_{cr}) the (re)orientation is enhanced and a transient current is emitted from the source that can be detected at the surface of the Earth (Varotsos and Alexopoulos, 1986).

(3) *Motion of segments of electrically charged dislocations upon sudden variations in local stress*: This model (Slifkin, this issue) makes use of the well-known phenomenon of the ionic electrical charge that resides on dislocations in non-metallic crystals in order to establish electrical equilibrium between the dislocation jogs and the point defects (e.g., vacancies and interstitial ions) in the bulk of the crystal.

In the following, we shall briefly describe the basic concepts of the above models and examine whether their predictions are compatible with the field SES data collected in Greece. For the case of the electrokinetic effect we shall only discuss the aspects developed by Gokhberg and co-workers because those of Morgan (1990), although extremely interesting, are not published separately in this volume.

6.1. SES generation according to the electrokinetic effect

According to Dobrovolsky et al. (1989) and Gershenzon et al., (1990) the preseismic electrotelluric field disturbances can be explained by

the electrokinetic (EK) effect; they are the result of strain changes affecting fluid dynamics taking place at the measurement site itself or around it.

The crust contains water-filled pore space (cracks and cavities) in practically all areas. A change in the cubic strain within the crust produces changes in the fluid pore pressure. An anisotropic increment in the pressure develops as a result of an inhomogeneous strain field. In other words, processes in the seismic source region at the final stage of earthquake preparation produce strain changes in areas that can extend for tens or hundreds of kilometres, depending on the magnitude of the impending earthquake. These rapid strain changes produce, under suitable conditions, through the electrokinetic process, local (i.e., close to the measuring site) electric fields which act as a mechano-electric transducer. In an homogeneous medium, and for any strain, the horizontal component of the electric field at the surface is zero. A non-zero electric field can arise at the surface only close to inhomogeneities in the electrophysical properties (Nourbehecht, 1963) close to measuring electrodes. According to this model, although the change in the crustal state of stress and strain before an earthquake extends for some tens or hundreds of kilometres, the electric field of electrokinetic origin arises locally at inhomogeneity sites and hence produces local electric fields of arbitrarily small dimensions, down to the electrode size.

Within the framework of the above model, the following remarks can be made on various physical properties of the preseismic electric variations:

(1) *Starting time and duration of a preseismic electric disturbance according to the EK model*: Fluid dynamics in a porous medium are described by an equation of the parabolic type, that is the pressure varies according to the diffusion law. Therefore, depending on the typical dimensions of the inhomogeneity and permeability in the medium, the duration of the electric field disturbance arising from a rapid (δ shaped) strain variation may vary from 1 min to 1 yr because, even after the disappearance of the strain, the electric field remains as it is, controlled by the

gradient of the pore pressure rather than the strain itself.

The starting time and the duration of the electric disturbance can depend on the location of the electrodes in relation to the inhomogeneity. For example, if both electrodes of a dipole lie on the same side of an interface (e.g., a vertical plane separating rocks with different properties), the electric field anomaly will have a ratio of time lag versus the strain which depends on the rate of fluid diffusion across distances comparable with that from the nearest electrode to the interface. Therefore, this time lag could vary, (from, for example, a few hours to several days). As a consequence of this, the electric field anomaly should be (in some cases) detected at different times on different dipoles of a given station (and, of course, at different times at different stations).

(2) *Dependence of the signal amplitude on the length of a dipole according to the EK model:* In an homogeneous medium, the potential difference $\Delta\varphi = \varphi_1 - \varphi_2$ between two sites 1 and 2 is controlled by the difference in the excess (super-hydrostatic) pore pressure, P , at these two sites:

$$\Delta\varphi = C(P_1 - P_2) \quad (1)$$

where C is the streaming potential coefficient. In cases, however, where the sites lie in rocks with different streaming potential coefficients (C_1 and C_2), the potential difference, $\Delta\varphi$, is given by (Fitterman, 1979):

$$\Delta\varphi = \Delta C \times \Delta P \quad (2)$$

where ΔP denotes the pore pressure change and $\Delta C = C_1 - C_2$.

We therefore discriminate two cases:

(a) *Homogeneous medium:* the fluid pressure at the surface itself is equal to the atmospheric pressure, so that no difference in pressure can develop. Therefore, eqn. (1) reveals that horizontal electric dipoles with electrodes at the Earth's surface should not record any preseismic electric anomaly. However, preseismic electrical anomalies can be recorded at vertical electric dipoles as follows: at the surface the excess pressure is always zero but at points within the crust strain changes will produce changes in the pressure and, hence, a potential difference will result be-

tween a point at surface and another at depth h (e.g., in a well, provided that the latter electrode lies below the water level and is covered with earth, making the pressure of the pore fluid around it such as it would have been, if there were no well at all). The $\Delta\varphi$ value is not proportional to h ; (Dobrovolsky et al., 1989): only the duration of the anomaly depends on h .

(b) *Measurements close to an inhomogeneity:* according to eqn. (2) and the aforementioned remarks, the jump on the potential difference between the electrodes (i.e., the preseismic electrical anomaly) is governed by the strain distribution and the electrode location relative to the inhomogeneity boundary; it does not depend on the length of the measuring dipole, it is only when the electrodes are situated on different sides of the inhomogeneity boundary, and when the distance from the boundary to the nearest electrode is appreciably smaller than the length of the boundary, but appreciably larger than the water level depth, that the length of the measuring dipole becomes important. In a case when both electrodes are situated on one side of an inhomogeneity, the signal amplitude does depend on the dipole's length, L ; the exact form of this dependence, however, changes with the geometry of the inhomogeneity and the situation of the electrode. When the distance between the inhomogeneity boundary and electrodes is much larger than the characteristic size of the inhomogeneity, the signal amplitude is proportional to L , but the signal will be small as it decreases with the distance, r , from the inhomogeneity according to a r^{-3} law. Of course, if there are sharp interfaces and large contrasts between rock properties, a larger $\Delta\varphi$ value is to be anticipated.

(3) *Comparison of the suggestions of the model for the electrokinetic effect with SES experimental results:* Although a number of the physical properties of the SES observed in Greece exhibit behaviour compatible with the model of Dobrovolsky, et al. (1989) (hereafter called DGG), there is also a number of experimental observations that contradict the DGG expectations.

(a) Our records show that the duration of SES may vary from 1 min to several hours, which is compatible with the DGG model.

(b) Our data indicate that the SES are simultaneously recorded (and have the same duration) at both the short and the long dipoles of the same station since the electrodes of these two types of dipoles lie kilometres apart (and, of course, at different distances from an inhomogeneity), we see that this behaviour is compatible with the DGG model only when some special conditions are fulfilled (Gershenzon, pers. commun., 1990). The model, in general, predicts that the starting time and the duration of the SES should depend on the location of the electrodes relative to the inhomogeneity.

(c) The DGG model emphasizes the role of inhomogeneities on SES detection; this expecta-

tion is in accordance with the local characteristics of the selectivity effect described in Paper I, in which inhomogeneities (e.g. dykes) provide localities that act as "amplifiers" for SES collection. In such cases, and in the vicinity of the inhomogeneity, the ΔV value of an SES is not found to be proportional to the length of the dipole (e.g., Fig. 20); this agrees with the DGG model.

(d) For dipoles lying far from strong inhomogeneities (such as dykes) the SES are found to have ΔV values proportional to the length L ; this observation can be explained by the DGG model, but, as mentioned, only under very special conditions.

(e) Concerning the form of the SES, it may

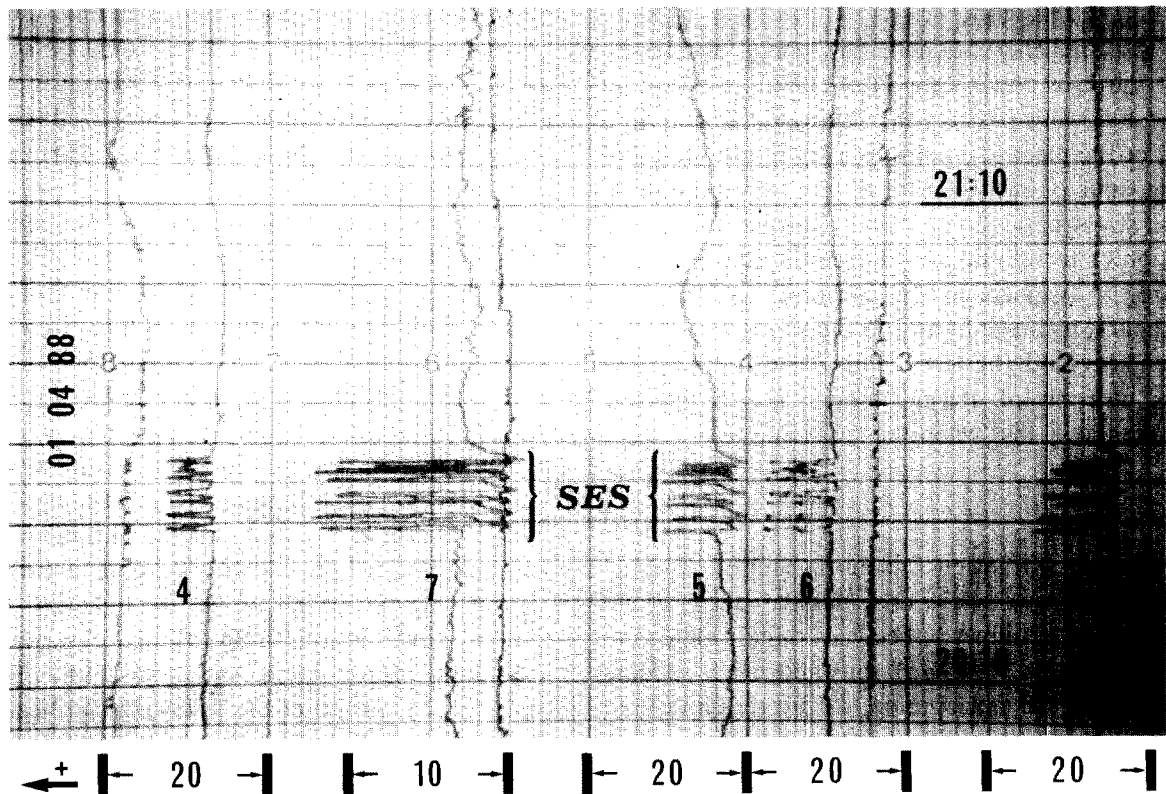


Fig. 20. Detection of an unusual SES series at station KER dipoles of various lengths close to and far away from a dyke with surface dimensions of the order of some metres. Dipoles labelled 5 and 8 have lengths of 1.5 and 1.1 km with one (not common) of their electrodes in the same dyke. The other electrode of dipole 5 lies on marble, whereas that of dipole 8 on granodiorite. Dipole 7 has a length of some metres and one of its electrodes lies within the aforementioned dyke whereas the other is placed just outside it several metres away. Dipole 6 has a length of around 1.1 km and has one of its electrodes on the dyke mentioned before, whereas the other electrode lies on another dyke. Dipole 4 is almost the same, as dipole 6 but its electrodes lie just outside the two dykes. Dipoles 4, 5, 6 and 8 are almost parallel to the N-S direction. This SES activity was followed by seismic activity only a few tens of kilometres northwest of the station; the two largest earthquakes in this sequence occurred: (1) at 20:06 GMT on April 2nd, 1988, at 38.0°N, 23.9°E, with $M_s = 4.3$ and (2) at 21:58 GMT on April 2nd, 1988, at 38.2°N, 24.1°E, with $M_s = 4.8$. Note that dipole 7, in spite of its very small length, has a ΔV value comparable to (and even larger than) those of the other dipoles that had lengths of over 1 km. This effect was discussed in detail in Paper I.

have a gradual or an abrupt (i.e., 20 sec) onset and a gradual or abrupt cessation. The combination "gradual onset/abrupt cessation" has never been observed. The latter experimental fact is correctly predicted by the DGG model; it *cannot* explain, however, the appearance of signals of short (i.e. a few minutes) duration, such as those observed before the Killini-Vartholomio destructive earthquakes (Figs. 8–10).

(f) The $\Delta\varphi$ values calculated from the DGG model are actually compatible with the ΔV values (for $L = 100$ m) of SES measured in Greece.

6.2. SES generation and transmission according to the model of piezo-stimulated currents

As already mentioned, this model, developed by Varotsos and Alexopoulos (1986), is based on the following picture: the relaxation time τ (T , P) of the electric dipoles existing in the preparation zone of an EQ changes with the variation in the stress applied (to a first approximation, and in order to simplify the discussion, the temperature is assumed to be constant); in the last preparatory stage of an EQ the stress varies continuously and the stress rate $b \equiv d\sigma/dt|_{\tau}$ may not be constant. It can be generally shown (see Appendix I) that when the relation:

$$\left. \frac{d\tau}{dt} \right|_{\tau} \approx -1$$

is fulfilled, a transient current is emitted. From a physical point of view, this emission occurs when the relaxation time, τ , becomes quite small (at a certain critical value σ_{cr}), thus allowing a sudden change in the polarization, Π ; by recalling that the time derivative of Π is the current density j ($= d\Pi/dt$) we see that a transient change of j (i.e., an SES) can be, in principle, detected at the surface of the Earth.

We turn now to the investigation of the following fundamental points: (1) whether this piezo-stimulated current (source) model can explain the "selectivity phenomenon" and (2) whether the observed SES values (i.e., $1 \text{ mV}/100 \text{ m} \approx 10^{-5} \text{ V/m}$), are compatible with reasonable (i.e., physically accepted) values of the current density generated at the source.

Concerning the selectivity-phenomenon, the data presented in Paper I support the opinion that it is a superposition of the following three factors: "source properties", "path" between the source and the station and "inhomogeneities" in the vicinity of the station. This superposition reveals that a "channel" might "drive" the "signal" from the source to the surface of the Earth as follows: the electric current is "concentrated" in a conductive channel (i.e., more conductive than the surroundings) that connects the source to the area of the station sensitive to SES. The current density is thus enhanced at the conductive channel; furthermore, the electric field is amplified if it meets a highly resistive anomaly, such as a dyke (Varotsos and Lazaridou, 1991), at the station. Within such a scheme, a station could be sensitive to a given seismic source only when it is close to a conductivity channel that connects this particular source with the surface of the Earth (see also appendix IV).

We now proceed to investigate the current density at the source necessary to give electric field values at the surface of the Earth of the order of 10^{-5} V/m . Utada (this issue) has already indicated that, when assuming the resistivity and the thickness of the conductivity channel to be $10 \text{ } \Omega\text{m}$ and 100 m , respectively, and an amplification factor of 100 (due to the surface resistivity anomaly) the source current intensity is only of the order of 10 A . Such a current is not unexpected because it corresponds to a current density of the order of $10 \text{ A}/1 \text{ km}^2 \approx 10^{-9} \text{ A/cm}^2$, which is comparable to that observed in laboratory measurements with rocks (10^{-9} – 10^{-8} A/cm^2). At this point the following clarification is necessary. Some of the literature precludes any possibility of the observed SES having been emitted from a current source close to the focal area. The argument is supported by applying the formula:

$$\epsilon = \frac{Il\rho}{4\pi r^3}$$

and using the values $\epsilon = 10^{-5} \text{ V/m}$ (experimental value from SES field measurements); $l \approx 1 \text{ km}$ (linear dimension of the emitting source); $\rho \approx 10^3$ – $10^2 \text{ } \Omega\text{m}$; to obtain a current intensity, I , of

the order of 10^5 – 10^6 A. Such values are actually very large. This argument ignores the following fundamental point: the above formula only holds for a uniform resistivity, ρ , which is not the case for the earth. Our data indicates that inhomogeneities play a major role in the transmission and collection of SES (e.g., the selectivity phenomenon is a result of these inhomogeneities). Furthermore, there are two independent experimental results that support our opinion:

(1) Park and Fitterman (1990) in Parkfield ejected rectangular current pulses ($I \approx 10$ A, $l \approx 1$ km) into the earth and observed that, at distances of between 10 and 100 km, some dipoles show null measurements whereas other ones (at comparable distances) did not. They also clarified that the orientation was not a major factor in these null measurements and concluded that they were due to a heterogeneous electrical structure. This result agrees with our field observations, that although one (Varotsos and Alexopoulos, 1984b) station is able to collect SES well above the noise level, from a given seismic area, another station, which lies at a comparable epicentral distance, may not be able to record the same SES at all.

(2) Soviet experiments with high power generators have shown that, by ejecting rectangular current pulses of the order of 10^4 A ($l = 1$ km), the corresponding disturbances can be recorded at great distances, or around 300 km, with electric field values comparable to our SES observations. These experiments undoubtedly show that current densities a few orders of magnitude smaller than the 10^6 A calculated theoretically can actually travel over long distances through inhomogeneities.

6.3. SES generation according to the charged dislocations model

Slifkin (this issue) has suggested that a possible mechanism for SES generation is the displacement of segments of charged dislocations responding to changes in the applied stress. Attention is drawn to the fact that this model enables the explanation of the generation of an electric signal, even in the absence of any fracture, as a

result of the bowing out of dislocation segments between pinning points. By using reasonable values for the parameters involved (dimensions of the source, density of the excess dislocations, etc.), Slifkin calculated an electric signal at the surface of the Earth comparable to that observed experimentally. For details of this model see Slifkin (this issue).

7. Outlook for the future: problems to be solved

Although other types of electrical precursors are promising, for the short term prediction of seismic events, it seems that only the SES contain the necessary information that, in principle, allows the prediction of the parameters of the impending events. The following suggestions for further experimentation refer to the current research carried out in Greece and, of course, do not represent our considerations concerning a complete earthquake prediction program.

7.1. Intensive experimentation on the sites that were found in Greece to be appropriate for SES collection

This experimentation should involve:

(1) Continuation of the stations already operating, in order to increase our knowledge on the selectivity properties of these sites.

(2) Detailed study of the geoelectrical structure, with MT measurements not only in the immediate vicinity of the stations, but also at other sites in the same area. Such a study will shortly start in collaboration with the Seismological Department of Uppsala University. After obtaining better knowledge of the structure of the total area, a number of new permanent dipoles should be installed at various sub-areas in order to investigate at which sites the SES are enhanced or disappear. This investigation is important because, as already mentioned, the selectivity depends simultaneously on source properties, the travel path and the inhomogeneities in the vicinity of the station. The influence of the latter factor can be isolated from the other two by studying the simultaneous SES at a number of sub-areas belonging to the same area, which, however, should lie far away from a seismic area.

For example, we consider out such a study at various sites around station IOA for carrying the EQs from Cephalonia, which have an epicentral distance of around 150 km.

(3) Spectrum analysis of SES. In Paper I it was mentioned that SES originating from the same seismic area and being detected at the same station occasionally have strikingly similar shapes. Therefore, a spectrum analysis of SES should be carried out in order to investigate whether some spectrum characteristics are correlated with the focal characteristics. If such a correlation exists, it might be used for an improvement of the accuracy of the prediction of the epicentre.

For a more reliable spectrum analysis, the current sampling rate during SES collection should be increased to a few tens of samples per second. This increase seems to be especially necessary for cases like those of SES shown in Figures 9, 10 and 17.

(4) Improvement of the accuracy in predicting the epicentre. The current procedure for predicting the epicentre from the SES data collected at a single station was described in Paper I and is based on a combination of the following information:

- (a) the selectivity map;
- (b) the polarity of the SES components;
- (c) the ratio $\Delta V_{EW}/\Delta V_{NS}$ (for $L = \text{constant}$) of the short dipoles.

Besides the obvious necessity of a better completion of the selectivity map, and an increase in the number of observation sites, the following complementary information could be helpful for improving the prediction accuracy:

(a) The value of the SES vertical component: preliminary measurements in the station KER, as mentioned in Paper I, have already showed a significant $\Delta V/L$ vertical value. Furthermore, measurements by our group at Zakynthos island, in boreholes with a depth of 200 m, verified the existence of a vertical component (Antonopoulos et al., this issue), only in a few cases. As the significance of the vertical component is expected to increase for stations close to inhomogeneities, we should investigate whether its ratio over the two horizontal components could correlate with the epicentral area.

(b) Installation of more long dipoles in various directions: when an SES is simultaneously recorded at a number of long dipoles, it is similar to having a number of neighbouring stations collecting the same SES. Note that in an inhomogeneous area the short-dipole values $\Delta V/L$ (E-W) and $\Delta V/L$ (N-S) of an SES do not generally reproduce the SES (average) $\Delta V/L$ values of the long dipoles in various directions. Therefore the latter values provide *complementary* information which could be used in the identification of the epicentre.

7.2. Experimentation at other sites

New stations, selective to SES, from various seismic areas of Greece should be found. This is not only important for the improvement of the accuracy of the prediction of parameters of the impending event, but also for understanding: (1) the correlation of the selectivity phenomenon with the geology and tectonics; (2) the conditions under which SES can be simultaneously recorded at remote stations, etc.

SES experimentation in other countries is also highly desirable in order to examine whether different geological environments affect the SES characteristics. SES studies in Japan by Uyeda and co-workers have shown that the form of the SES and the time lag between SES and EQs is comparable with those observed in Greece, (Kinoshita et al., 1989; Kawase et al., this issue).

Appendix I: Comments on the pressure stimulated currents (PSC)

As described in Varotsos and Alexopoulos (1986), the pressure stimulated currents (PSC) are transient currents that are emitted from a solid containing electric dipoles upon a gradual variation of the pressure. The PSC can be detected either by increasing or by decreasing the pressure, depending on whether the so-called migration volume, v^d (defined below), for the (re)orientation of the dipoles is negative or positive. From a physical point of view, a negative value of v^d means that, upon increasing pressure the relaxation time, τ , of the dipoles becomes

smaller, whereas the opposite holds for $v^d > 0$. This is obvious from the relation:

$$\tau = (\lambda\nu)^{-1} \exp\left(\frac{g}{kT}\right) \quad (\text{A.1})$$

where λ = the number of jump paths accessible to the jumping species with an attempt frequency ν , and G = the Gibbs energy for the (re)orientation process.

The migration volume, v^d , is defined as:

$$v^d = \left. \frac{dG}{dP} \right|_T \quad (\text{A.2})$$

and hence eqn. (A.1) indicates that the pressure variation of τ depends exclusively on the sign of v^d , because the frequency ν usually varies only slightly with pressure (Varotsos and Alexopoulos, 1980).

The PSC are classified into two categories: pressure stimulated polarization currents (PSPC) and pressure stimulated depolarization currents (PSDC). The former refers to the polarization that arises when the relaxation time becomes (under a gradual variation of pressure) sufficiently small, so that the dipoles align from a random orientation into the direction of a continuously acting electric field (external or internal one). In the second technique a body is initially brought into a fully polarized state, which can be achieved by an external field under conditions of relatively fast relaxation. If a change in pressure then increases the relaxation time (to a relatively high value) and the field is subsequently switched off, the body will remain in a practically fully polarized state. A depolarization current will be measured if the aligned dipoles can turn into random directions; this, in the absence of an electric field, occurs in a form of a current pulse when the relaxation time becomes sufficiently small. This will occur when the change in the pressure is reversed.

Condition at which the PSC maximizes: As a general statement, we can say that the observation of PSC is made when changing the pressure towards the direction that decreases the relaxation time of the dipoles. It will be shown below that the current density of the PSC reaches its maximum (absolute) value J_M at a critical pres-

sure P_{cr} for which, irrespective of the sign of the volume v^d , the following relation holds:

$$\frac{bv^d}{kT} = -\frac{1}{\tau(P_{cr})} \quad (\text{A.3})$$

where b = the rate of the pressure variation; and $\tau(P_{cr})$ = the value of the relaxation time when $P = P_{cr}$.

For one type of non-interacting dipole and a single (re)orientation mechanism we can write (for the case of PSDC):

$$J = \frac{d\Pi(t)}{dt} = -\frac{\Pi(t)}{\tau} \quad (\text{A.4})$$

where J = the current density; and $\Pi(t)$ = the polarization. Equation (A.4) leads to:

$$J\tau = -\Pi(t)$$

and differentiating with respect to time:

$$J \left. \frac{d\tau}{dt} \right|_T + \tau \left. \frac{dJ}{dt} \right|_T = - \left. \frac{d\Pi(t)}{dt} \right|_T$$

or, in view of eqn. (A.4):

$$J \left. \frac{d\tau}{dt} \right|_T + \tau \left. \frac{dJ}{dt} \right|_T = -J \quad (\text{A.5})$$

The maximum current, J_M , occurs at a pressure $P = P_{cr}$ for which:

$$\left. \frac{dJ}{dt} \right|_{J=J_M} = 0$$

and then eqn. (A.5) gives:

$$\left. \frac{d\tau}{dt} \right|_{T, J=J_M} = -1 \quad (\text{A.6})$$

or:

$$\left. \frac{d\tau}{dP} \right|_{T, J=J_M} \left. \frac{dP}{dt} \right|_{T, J=J_M} = -1$$

or:

$$b \left. \frac{d\tau}{dP} \right|_{T, J=J_M} = -1 \quad (\text{A.7})$$

where b = the rate of the pressure variation.

By differentiating eqn. (A.1) in respect to pressure we get:

$$\begin{aligned} \left. \frac{d\tau}{dP} \right|_T &= (\lambda\nu)^{-1} \exp\left(\frac{G}{kT}\right) \frac{1}{kT} \left. \frac{dG}{dP} \right|_T \\ &+ \lambda^{-1} \exp\left(\frac{G}{kT}\right) \left. \frac{d(\nu^{-1})}{dP} \right|_T \end{aligned} \quad (\text{A.8})$$

For reasons explained by Varotsos and Alexopoulos (1980, 1986) the last term of eqn. (A.8) can be disregarded; furthermore, by inserting eqns. (A.1) and (A.2) into eqn. (A.8) we get:

$$\left. \frac{d\tau}{dP} \right|_{T, J=J_M} = \tau(P_{cr}) \frac{v^d}{kT}$$

In view of the latter relation, eqn. (A.7) gives:

$$-\frac{bv^d}{kT} = \frac{1}{\tau(P_{cr})} \quad (\text{A.9})$$

This is the condition that holds at the appearance of the maximum (absolute) value J_M of the PSDC. In a similar fashion, this relation (except for an additional correction term on the right side that is usually negligible) can also be proved for the case of PSPC. It should be clarified that the value on the left side is always positive because, whenever v^d is negative, the PSC is observed upon increasing pressure (and then the value of b is negative). Furthermore, we should emphasize that eqn. (A.9) was derived *without* assuming that b remains constant during the experiment.

Variation in the pressure P_{cr} (at which the PSC maximizes) for different pressure rates: Equation (A.9) reads:

$$b(P_{cr}) = -\frac{kT}{\tau(P_{cr})v^d}$$

$$b(P_{cr}) = -\frac{kT\lambda\nu}{v^d} \exp\left[-\frac{G(P_{cr})}{kT}\right] \quad (\text{A.10})$$

In order to investigate how P_{cr} varies as a function of b we differentiate eqn. (A.10) with respect to P_{cr} . We finally get:

$$\left. \frac{db(P_{cr})}{dP_{cr}} \right|_T \approx \frac{1}{\tau(P_{cr})} \quad (\text{A.11})$$

This relation shows that the derivative:

$$\left. \frac{db}{dP_{cr}} \right|_T$$

is always positive. The following two cases can be determined:

(1) whenever v^d is positive the PSC is released upon decreasing the pressure from an initial pres-

sure, P_i , to a pressure P_{cr} (determined from eqn. (A.9)); that is, the rate b is negative; in this case the positive value of the derivative:

$$\left. \frac{db}{dP_{cr}} \right|_T$$

means that, when the absolute value of the rate increases then the pressure P_{cr} moves towards lower values;

(2) whenever v^d is negative, the PSC is released upon increasing pressure, that is, rate b is positive; therefore the inequality:

$$\left. \frac{db(P_{cr})}{dP_{cr}} \right|_T > 0$$

shows that, when rate b becomes larger, the pressure P_{cr} increases.

Implications of the aforementioned PSC properties to the SES model proposed by Varotsos and Alexopoulos (1986): This model suggests, as mentioned, that, during the last preparatory stage of an EQ, PSPC is emitted from the focal area; it is assumed that the v^d value is negative and that the fracture stress, P_{fr} , is larger than the (critical) stress value, P_{cr} , at which the PSPC is emitted.

It has been observed that even for a given area the time lag, Δt , between SES and EQs varies by two orders of magnitude: between a couple of hours and a few weeks; this non-constancy of Δt might be explained as follows: we can always write:

$$P_{fr} - P_{cr} = \int_{P_{cr}}^{P_{fr}} b \, dP$$

which turns to:

$$\Delta t = \frac{P_{fr} - P_{cr}}{b} \quad (\text{A.12})$$

if the value of b is assumed to remain constant when the stress gradually increases during the last preparatory stage of a given EQ. For another EQ from the same area the P_{fr} could be assumed to be the same, while the b value might be different. In such a case, a larger rate of b would reflect a greater P_{cr} , thus leading (according to eqn. (A.12)) to a smaller Δt .

Appendix II: recognition of anthropogenic noise

It is often difficult to decide if a fluctuation in the telluric field is a SES or is due to noise. The procedure according to which an SES can be discriminated from various types of noise (electrochemical, magnetotelluric and anthropogenic) has been described in detail in Paper I. Here we shall only indicate how anthropogenic noise can be discriminated when originates repeatedly from the same point. In such cases the comparison of the registrations on two parallel dipoles of different lengths allows a decision to be made when the electrodes are suitably positioned in relation to the noise source.

Let us consider the electrodes e and w of the short dipole and E and W of the long dipole, which lie on a straight line in the direction east-west and a noise source, N that lies on this line. The current of N is assumed to travel in all directions and to consist of negative charges, so that the potential difference in regard to N will have the general form given in Figure 21. If point N happens to lie near W (case I) then the potentials V_w , V_E , v_w and v_e fulfil the conditions: $V_E > V_w$ and $v_e > v_w$. Therefore, disturbances arising from the noise source N will have the same polarity on both dipoles (EW and ew), a situation similar to the SES. If, on the other hand, point N lies near to the other three electrodes (case II) the potentials give $v_e > v_w$ and $V_E < V_w$; in this case we see that the polarity of the noise signal on the short dipole is opposite to that on the long one. Thus signals of different polarities on the dipoles ew and EW cannot be

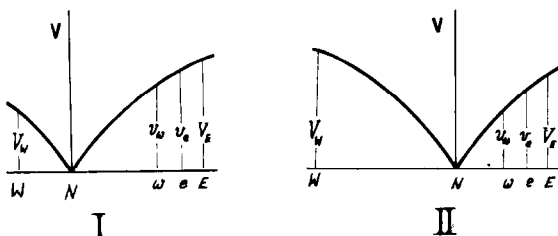


Fig. 21. In configuration I a disturbance from noise source N (or an SES) is recorded on both dipoles ew and EW , with the same polarity. In case II, a disturbance from N give signals of different polarities on the dipoles ew and EW , in contrast to an SES.

true SES. Therefore, *configuration II is recommended* for easy discrimination between noise and true SES.

Appendix III: predictions issued by the VAN telemetric network

Prior to the occurrence of the earthquakes, predictions were announced by telegrams sent to the Greek Government. Each telegram usually contains the following information:

- (1) station(s) at which the SES were recorded;
- (2) arrival time of the SES;
- (3) location of the predicted epicentre given by the epicentral distance(s) (in kilometres) and the direction with regard to Athens;
- (4) estimation of the surface wave magnitude, M_s , of the impending earthquake. (Magnitudes are reported in the Preliminary Seismological Bulletin (PSB) of the Seismological Institute of the National Observatory of Athens (SI-NOA); in cases where M_s values are not reported they are estimated by means of the approximate formula $M_s \approx M_L + 0.5$. We draw the attention to the fact that the M_s values reported by the PSB of SI-NOA exceed the magnitude values reported by the USGS catalogue by 0.3 or more (Uyeda, 1991; Hamada, this issue));
- (5) a statement clarifying whether the prediction refers to a single SES or a sequence of SES called electrical activity. This clarification is essential because, as mentioned in the Introduction, it indicates the time window of the expected earthquake(s).

Since May 15th, 1988, all telegrams were sent not only to the Greek Government but also to Scientific Institutes in other countries (such as the USA, Japan, France and Sweden).

Applying an official decision in 1985, predictions were issued only when the impending earthquake was expected to cause some damage, that is, when the predicted M_s value was 5.0 or larger. A list of all the predictions issued during the 3-yr period 1987–1989 can be found in the paper by Varotsos and Lazaridou (1991; copies of them are also given in Dologlou (this issue). Earlier predictions can be found in the papers by Varotsos and Alexopoulos (1984b) and by Varotsos et al. (1988).

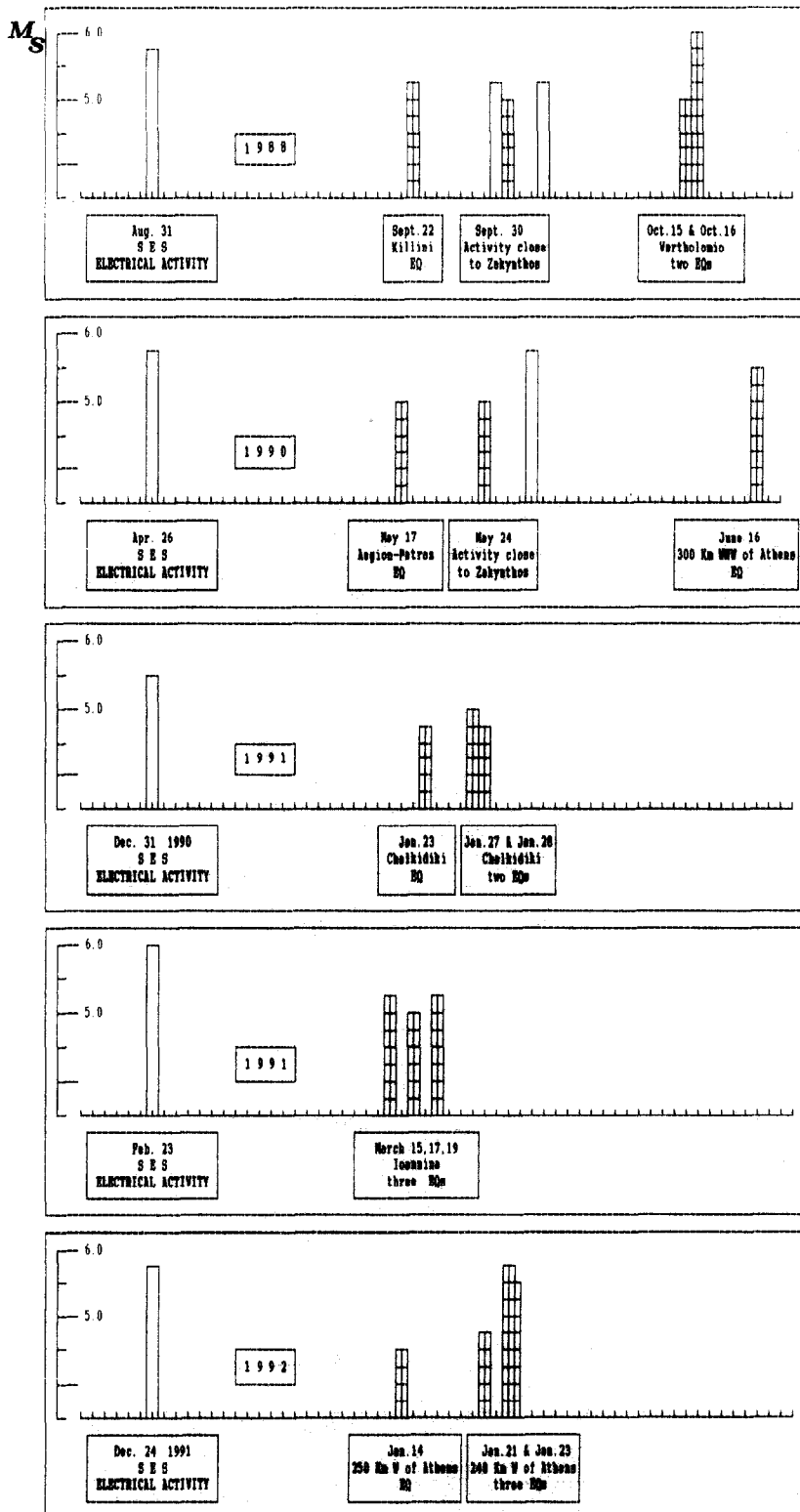


Fig. 22. Schematic comparison of five significant SES electrical activities recorded during the last 4 yrs. Note that the first strong EQ occurs 3 weeks after the SES activity, while small magnitude events (not shown in the figure) start earlier (usually within approximately 11 days).

Furthermore, the predictions issued after the preparation of this paper from February 6th, 1990, to May 31, 1992, are discussed in a recent paper by Varotsos et al. (1993). For the help of

the reader we give below a brief description of the latter predictions.

Statistical evaluation of the VAN predictions issued before the Athens Conference (February,

TABLE 3

All earthquakes with $M_B(\text{USGS}) \geq 5.0$ units, from January 1st, 1987 to January 31st, 1992, within the area N_{36}^{41} E_{19}^{25} excluding the EQs in Albania)

| Earthquake | | | | | Prediction | | | |
|-----------------------|---------------|---------------------------------|-----------------|----------------|-------------------------|--|--------------------|--------------|
| Date (DD-MM-YY) | Time (GMT) | Epicenter (USGS) (°N, °E) | M_B (USGS) | M_s (ATH) | Date (DD-MM-YY) | Epicenter and magnitude | Δr (km) | ΔM^d |
| 27-02-87 | 23:34 | 38.47, 20.29 | 5.3 | (5.9) | 26-02-87 | W 300 6.5 | 30 | -0.6 |
| 29-05-87 | 18:40 | 37.55, 21.57 | 5.2 | (5.5) | 27-04-87 ^a | 50 km from station PIR with M_s 5.5 | 30 | 0.0 |
| 10-06-87 | 14:50 | 37.23, 21.46 | 5.2 | (5.6) | 27-04-87 | 50 km from station PIR with M_s 5.5 | 30 | 0.1 |
| 18-05-88 | 05:17 | 38.42, 20.48 | 5.4 | (5.9) | 15-05-88 | W 300 5.3 or NW 330 5.0 | 30 | 0.5 |
| 22-05-88 | 03:44 | 38.41, 20.46 | 5.0 | (5.5) | 21-05-88 | W 300 5.3 | 30 | 0.2 |
| 05-07-88 | 20:34 | 38.15, 22.84 | 5.0 | (4.9) | Missed | - | - | - |
| 22-09-88 | 12:05 | 38.02, 21.09 | 5.0 | (5.1-5.5) | 01-09-88 ^b | W 240 5.8 or NW 300 5.3 | 20 | -0.5 |
| 16-10-88 | 12:34 | 37.84, 20.93 | 5.5 | (6.0) | 30-09-88 ^b | W240 5.3 or NW 330 5.0 | 20 | 0.7 |
| 19-03-89 | 05:36 | 39.25, 23.52 | 5.2 | (5.8) | Missed | - | - | - |
| 07-06-89 | 19:45 | 38.06, 21.62 | 5.0 | (5.2) | 03-06-89 | W300 5.5 or NW 350 5.0 | 120 | 0.3 |
| 20-08-89 | 18:32 | 37.28, 21.20 | 5.4 | (5.9) | 16-08-89 | WNW 200 5.0 | 120 | 0.9 |
| 24-08-89 | 02:13 | 38.00, 20.18 | 5.1 | (5.7) | 16-08-89 | WNW 200 5.0 | 120 | 0.7 |
| 04-02-90 | 02:30 | 37.47, 20.97 | 5.0 | (4.8) | Missed | - | - | - |
| 16-06-90 ^c | 02:16 | 39.26, 20.53 | 5.6 | (5.2) | 28-05-90 ^{b,c} | A displacement by a few tens of kms from the point W 240 is expected M_s 5.5 | 120-140 | -0.6 |
| 04-08-90 ^c | 07:29 | 39.32, 20.44 | 5.0 | (5.0) | Missed | - | - | - |
| 21-12-90 ^c | 06:57 | 41.00, 22.30 | 5.8 | (5.9) | Missed | - | - | - |
| 26-06-91 ^c | 11:43 | 38.43, 21.10 | 5.0 | (5.4) | Missed | - | - | - |
| 23-01-92 ^c | 01:23 | 38.31, 20.54 | 5.1 | (5.5) | 27-12-91 ^b | W 240-5.7 | 30 | -0.2 |

^a Gradual variation in the electric field of the earth (GVEF, see text) that appears a couple of weeks before EQ with $M_s \geq 5.5$.

^b Cases of electrical activity described in detail in Fig. 2.

^c Prediction addressed directly to the Prime Minister.

^d $\Delta M = M_s(\text{ATH}) - M_{\text{predicted}}$.

^e Only four telemetric VAN stations (ASS, IOA, PIR and KER) were in operation.

1990): A detailed statistical treatment of the success rate, alarm rate and probability gain of the VAN predictions issued during the period 1987–1989 can be found in the paper by Hamada (this issue). Hamada (this issue) has shown that, for earthquakes with M_B (USGS) ≥ 5.0 , the ratio of the predicted to the total number of earthquakes is 6/12 (50%) and the success rate of the prediction is also 6/12 (50%), with a probability gain of a factor of 4. Furthermore, Hamada proved that, with a confidence level of 99.8%, it is not possible that this success rate can be explained by a random model of earthquake occurrence, taking into account a regional factor which includes high seismicity in the prediction area.

An independent statistical evaluation, using a different procedure has been carried out by the group working under Prof. Keilis Börok (Shnirman et al., this issue). They also dealt with the VAN predictions issued during the period 1987–1989 and concluded that, for the strongest magnitudes, there is an obvious correlation between the prediction telegrams and the earthquakes contained in independent earthquake catalogues (NOAA and EMSC).

Predictions issued after the Conference: Five predictions were issued during the period from February 6th, 1990, to February 6th 1992 the details of which are given in Varotsos et al. (1993). In addition to the official telegrams mentioned above, in three out of these five cases the predictions were submitted to *Tectonophysics* before the initiation of the corresponding seismic activity while in a fourth case the prediction was issued well in advance, during an International Conference held in Japan (Varotsos et al., 1991a, b). It is interesting to note that, out of these five, four predictions were based on electrical activities and were followed by a sequence of seismic events, the strongest of which are depicted in Figure 22. For the sake of comparison, we also insert in the same figure the case of the electrical activity that preceded the destructive earthquakes of Killini-Vartholomio during an earlier period in 1988. This comparison reveals the following points:

(1) The first strong earthquake occurs roughly 3 weeks after the initiation of the electrical activ-

ity: it occurred after 23 days in 1988, 21 days in 1990, 23 days and 20 days, respectively, for the two cases in 1991 and 21 days in 1992. As for the second significant earthquake it followed the first one with a delay of the order of 1 week.

(2) The study of the seismicity bulletins shows that small magnitude earthquakes actually started within about 11 days of the initiation of the SES activity.

If our observation in these five cases shown in Fig. 22 generally holds, the following conclusion might be drawn: in the case of the so-called electrical activity, strong earthquakes are preceded by weaker ones (i.e., foreshocks). In contrast, when the electrical disturbance consists of a single intense signal (i.e., SES) then the major event is not preceded by smaller shocks. It is a curious fact that the first strong earthquake in all five cases occurred 3 weeks after the electrical activity which, if true, reduces the time window of the first strong shock to a few days.

Summary of all the predictions issued to date: As already mentioned, a complete list of the telegrams issued during the 5 yr period January 1st, 1987, to February 6th, 1992, can be found in Varotsos and Lazaridou (1991) and Varotsos et al. (1993). However, for convenience, Table 3 lists all EQs with M_B (USGS) ≥ 5.0 which have occurred during this 5 yr period within the area N_{36}^{41}

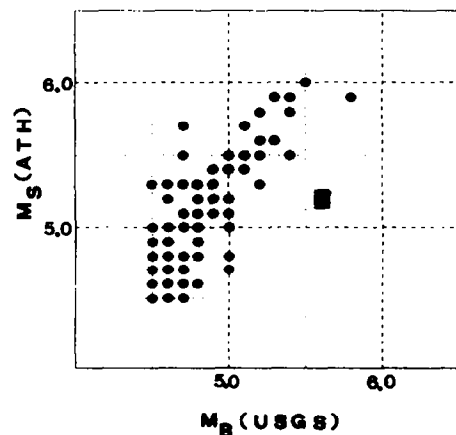


Fig. 23. Surface wave magnitude (M_s) values determined by Athens (ATH) Observatory versus the M_B values reported by the US Geological Survey (USGS). Note that, for $M_B > 5.0$, the difference M_s (ATH) – M_B (USGS) is around 0.5.

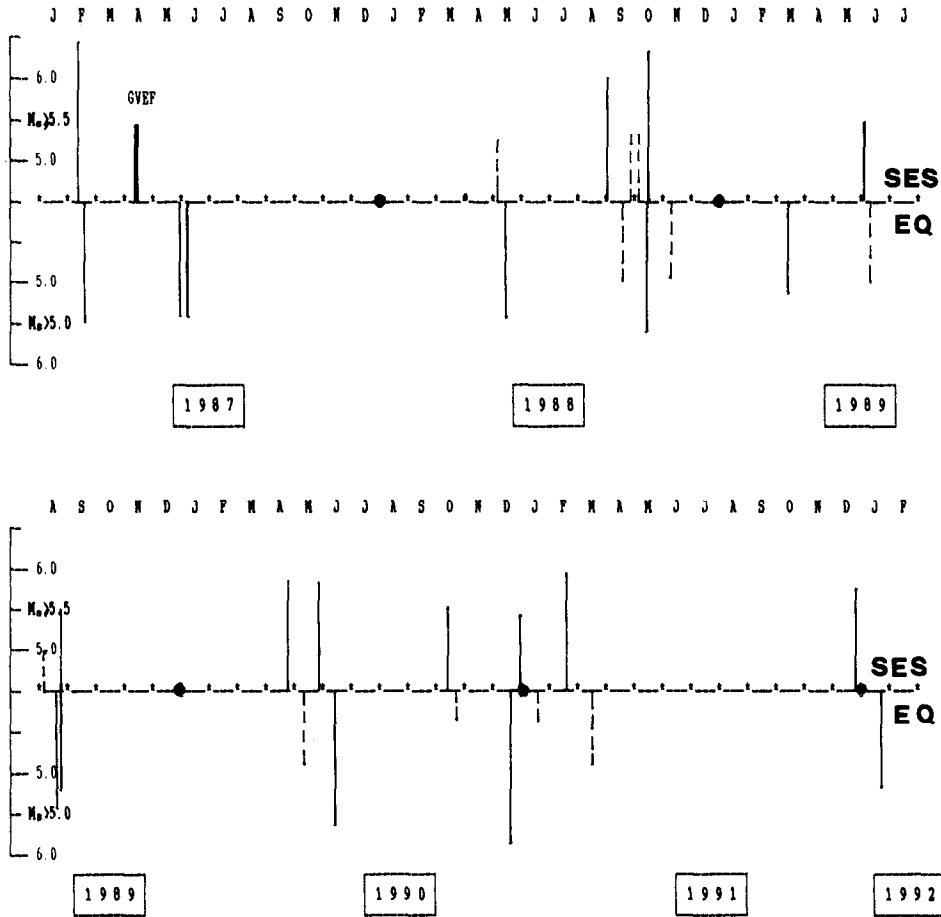


Fig. 24. Time chart of the 5 yr period from January 1st, 1987, to February 6th, 1992. The solid bars show all predictions (up) issued for an expected M_s (ATH) magnitude ≥ 5.5 and all EQs (down) with M_B (USGS) > 5.0 . (The dashed bars refer to lower magnitudes and have been added for clarity.)

E_{19}^{25} (excluding the EQs which occurred in Albania). In the same Table, the M_s values reported by the Athens (ATH) Observatory (i.e., by PSB of SI-NOA) are also given in parentheses, along with the predictions. The last two columns shows

the deviations, Δr and ΔM , between the predicted and the actual epicentral coordinates and magnitude, respectively.

In order to investigate the difference between the magnitude values reported by various Insti-

TABLE 4

Alarm rate for various magnitude thresholds for the period January 1st, 1987, to January 31st, 1992

| Magnitude ^a threshold | Total ^b number of EQs | Number of events missed | Number of successful predictions | | Alarm rate | |
|----------------------------------|----------------------------------|-------------------------|----------------------------------|-----------------------|------------------------|-----------------------|
| | | | $\Delta r \leq 120$ km | $\Delta r \leq 30$ km | $\Delta r \leq 120$ km | $\Delta r \leq 30$ km |
| $M_B > 5$ | 11 | 2 | 9 | 6 | 9/11 | 6/11 |
| $M_B \geq 5.3$ | 6 | 1 | 5 | 3 | 5/6 | 3/6 |
| $M_B \geq 5.5$ | 3 | 1 | 2 | 1 | 2/3 | 1/3 |

^a M_B values from the US Geological Survey.

^b All earthquakes within the area $N_{36}^{41} E_{19}^{25}$ (excluding those occurring in Albania).

tutes, Figure 23 shows a plot of the $M_s(\text{ATH})$ values compared to $M_B(\text{USGS})$. This figure indicates that, when M_B is larger than 5.0 the difference $M_s(\text{ATH}) - M_B(\text{USGS})$ is more or less systematic and lies around 0.5. (The only exception corresponds to the destructive EQ of June 16th, 1990—marked with a square in Fig. 23—for which the prediction was addressed directly to the Prime Minister on May 28th, 1990). In view of this result, and in order to visualize the correlation between SES and EQs more clearly Figure 24 shows a time chart, the solid bars of which show all EQs with $M_B(\text{USGS}) > 5.0$ (down) and all predictions issued with an expected magnitude $M_s(\text{ATH}) \geq 5.5$ (up) for the 5 yr period mentioned in Table 3.

Table 4 summarizes the results of various magnitude thresholds. It should be clarified that the only event with $M_B \geq 5.3$ that was missed is the EQ that occurred on December 21st, 1990; although for this EQ a clear SES was recorded at station ASS, no prediction could be issued because at that time only four stations (ASS, IOA, KER and PIR) in the SES network were in operation.

Appendix IV: additional comments on the theoretical models suggested for the explanation of SES generation

After the completion of the main text, Lazarus (this issue) suggested a pioneering model for SES generation, the main points of which are: during the preparation stage of an EQ, water must arise from hydrous-to-anhydrous transitions in ionic terrestrial minerals, caused by a build-up of hydrostatic pressure in the fault region when the pressure becomes sufficient, the hydrous solids must transform to anhydrous forms, with a sudden contraction in the lattice and release of the liquid water. This sudden contraction is accompanied by a large and sudden plastic deformation in the surrounding region, accompanied by the generation of large electrostatic signals (the SES). The SES, as a very low frequency signal, would propagate preferentially through regions of high dielectric constant between the source and detector. Ordinary water, with a dielectric constant of 80 at very low frequency, is a clear choice for the

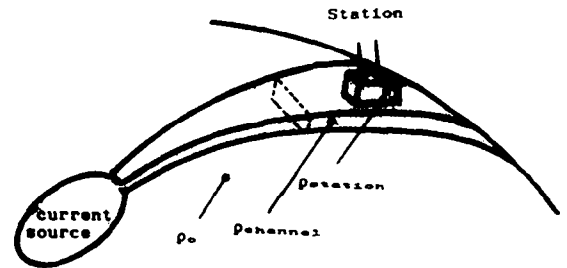


Fig. 25. Plausible explanation of the selectivity phenomenon on the basis of the model of piezo-stimulated currents suggested by Varotsos and Alexopoulos (1986). The current density is enhanced at a channel (e.g. a sufficiently wet path) which has a resistivity (ρ_{channel}) appreciably smaller than that of the surroundings (ρ_0) i.e., $\rho_{\text{channel}} \ll \rho_0$. The electric field is larger along the outcrop of this conductivity channel and is again amplified at a high resistivity anomaly lying along this outcrop. This resistivity anomaly is the correct place for the location of a station ($\rho_{\text{station}} > \rho_{\text{channel}}$) sensitive to those epicenters that correspond to the "current source" depicted in the figure.

formation of such regions and the long-distance SES propagation would depend on the prior existence of sufficiently wet paths between "preferred" epicenters and "sensitive" detector regions.

It is worthwhile remembering at this point that, as already discussed in the main text, according to the model of piezo-stimulated currents the existence of sufficiently wet paths between the (current) source and "sensitive" stations could lead to an explanation of the selectivity phenomenon (Fig. 25).

References

- Antonopoulos, G., Kopanas, J., Eftaxias, K. and Hadjiconis, V., 1993. On the experimental evidence of SES vertical component. *Tectonophysics*, 224: 47–49.
- Dobrovolsky, I.P., Gershenzon, N.I. and Gokhberg, M.B., 1989. Theory of electrokinetic effect occurring at the final state in the preparation of a tectonic earthquake. *Phys. Earth Planet. Inter.*, 57: 144–156.
- Fitterman, D.V., 1978. Electrokinetic and magnetic anomalies associated with dilatant regions in a layered earth. *J. Geophys. Res.*, 83 (B12): 5923–5928.
- Fitterman, D.V., 1979. Calculations of self-potential anomalies near vertical contacts. *Geophysics*, 44: 195–205.
- Gershenzon, N.I., Gokhberg, M.B., Kurshashov, Yu.P., Critkov, E.B., Cheruyi, V.I., Drumya, A.V. and Bogorodsky, M.M., 1990. On the generation of electrotelluric fields by crustal geodynamic processes. EMC'90 Int. Symp. on Electromagnetic Compatibility (Wroclaw, Poland).

- Hadjiannou, D., Vallianatos, F., Eftaxias, K., Hadjicontis, V. and Nomicos, K., 1993. Magnetotelluric noise subtraction from the VAN measurements. *Tectonophysics*, 224: 113–124.
- Hamada, K., 1993. Statistical evaluation of the SES-predictions issued in Greece: Alarm and success rates. *Tectonophysics*, 224: 203–210.
- Kawase, T., Uyeda, S., Uyeshima, M. and Kinoshita, M., 1993. Possible correlation between geoelectric potential change in Izu-Oshima Island and the earthquake swarm off east Izu Peninsula, Japan. *Tectonophysics*, 224: 83–93.
- Kinoshita, M., Uyeshima, M. and Uyeda, S., 1989. Earthquake prediction research by means of telluric potential monitoring. Progress Rep. 1: Installation of monitoring network. *Bull. Earthquake Res. Inst.*, 64: 255–311.
- Lazarus, D., 1993. Note on a possible origin for Seismic Electric Signals, *Tectonophysics*, 224: 265–267.
- Morgan, D., 1990. A model for the explanation of SES-generation based on electrokinetic effect. *Int. Conf. on Measurements and Theoretical Models of the Earth's Field Variations Related to Earthquakes* (Athens, February).
- Nourbehecht, B., 1963. Irreversible thermodynamic effects in inhomogeneous media and their applications in certain geoelectric problems. Ph.D. thesis, Massachusetts Inst. Technol., Cambridge, MA, USA.
- Parkhomenko, E.K., 1981. *Electrification Phenomena in Rocks*. Monographs in Geoscience. Plenum, New York.
- Park, S. and Fitterman, D., 1990. Sensitivity of the telluric monitoring array in Parkfield, California, to changes of resistivity. *J. Geophys. Res.*, 95: 15557–15571.
- Shnirman, M., Schreider, S. and Dmitrieva, O., 1993. Statistical evaluation of the SES predictions issued in Greece. *Tectonophysics*, 224: 211–221.
- Slifkin, L., 1992. Seismic Electric Signals from displacement of charged dislocations. *Tectonophysics*, 224: 149–152.
- Varotsos, P. and Alexopoulos, K., 1980. On the question of the calculation of migration volume in ionic crystals. *Philos. Mag.*, A42: 13–18.
- Varotsos, P. and Alexopoulos, K., 1984a. Physical properties of the variations of the electric field of the earth preceding earthquakes, I. *Tectonophysics*, 110: 73–98.
- Varotsos, P. and Alexopoulos, K., 1984b. Physical properties of the electric field of the earth preceding earthquakes, II. Determination of epicenter and magnitude. *Tectonophysics*, 110: 99–125.
- Varotsos, P. and Alexopoulos, K., 1986. Stimulated current emission in the earth: piezostimulated currents and related geophysical aspects. In: S. Amelinckx, R. Gevers and J. Nihoul (Editors), *Thermodynamics of Point Defects and their Relation with Bulk Properties*. North-Holland, Amsterdam, pp. 136–142, 403–406, 410–412, 417–420.
- Varotsos, P. and Alexopoulos, K., 1987. Physical properties of the variations of the electric field of the earth preceding earthquakes, III. *Tectonophysics*, 136: 335–339.
- Varotsos, P. and Lazaridou, M., 1991. Latest aspects of earthquake prediction in Greece based on seismic electric signals. *Tectonophysics*, 188: 321–347.
- Varotsos, P., Alexopoulos, K. and Nomicos, K., 1981. Seismic electric currents. *Prakt. Akad. Athenon*, 56: 277–286.
- Varotsos, P., Alexopoulos, K., Nomicos, K. and Lazaridou, M., 1986. Earthquake prediction and electric signals. *Nature*, 322: 120.
- Varotsos, P., Alexopoulos, K., Nomicos, K. and Lazaridou, M., 1988. Official earthquake prediction procedure in Greece. In: O. Kulhanek (Editor), *Seismic Source Physics and Earthquake Prediction Research*. *Tectonophysics*, 152: 193–196.
- Varotsos, P., Alexopoulos, K. and Lazaridou, M., 1991a. Comments on the recent Seismic Electric Signal activity in Greece. *Proc. Int. Seminar on Earthquake Prediction and Hazard Mitigation Technology* (Tsukuba, March 5–8, 1991) pp. 323–331.
- Varotsos, P., Alexopoulos, K. and Lazaridou, M., 1991b. *News. Jpn. Seism. Soc.*, 3 (4): 26–29.
- Varotsos, P., Alexopoulos, K., Lazaridou, M. and Nagao, T., 1993. Earthquake predictions issued in Greece since February 6, 1990. *Tectonophysics*, 224.
- Uyeda, S., 1991. Greece; A country where earthquake prediction is in practice. *Zisin*, 44: 391–405.